

Structural and Chemical Effects of the P^tBu₂ Bridge at Unsaturated Dimolybdenum Complexes Having Hydride and Hydrocarbyl Ligands

M. Angeles Alvarez, Melodie Casado-Ruano, M. Esther García, Daniel García-Vivó, Miguel A. Ruiz**

Departamento de Química Orgánica e Inorgánica/IUQOEM, Universidad de Oviedo, E-33071 Oviedo, Spain.

Abstract

A high-yield synthetic route for the preparation of the unsaturated anion [Mo₂Cp₂(μ-P^tBu₂)(μ-CO)₂]⁻ (**2**) was implemented, via two-electron reduction of the chloride complex [Mo₂Cp₂(μ-Cl)(μ-P^tBu₂)(CO)₂] (**1**). Reaction of **2** with [NH₄][PF₆] led to the formation of the 30-electron complex [Mo₂Cp₂(H)(μ-P^tBu₂)(CO)₂] (**3**), in which the hydride ligand adopts an uncommon terminal disposition. DFT analysis of the electronic structure of **3** gave support to the presence of a M-M triple bond in this complex following from a σ²δ²δ² configuration, a view also supported by the high electron density accumulated at the corresponding Mo–Mo bond critical point. In contrast, reactions of **2** with IMe or ClCH₂Ph gave the alkyl-bridged complexes [Mo₂Cp₂(μ-κ¹:η²-CH₂R)(μ-P^tBu₂)(CO)₂] (R = H (**4a**), Ph (**4b**)), which in solution display agostic Mo–H–C interactions. Decarbonylation of **4a** took place rapidly under photochemical conditions to give the 30-electron complex [Mo₂Cp₂(μ-κ¹:η²-CH₃)(μ-P^tBu₂)(μ-CO)] (**7**), with a stronger agostic coordination of its methyl ligand. In contrast, irradiation of **4b** led to the formation of the benzyldiyne derivative [Mo₂Cp₂(μ-CPh)(μ-P^tBu₂)(μ-CO)] (**9**), following from fast decarbonylation and dehydrogenation of the bridging benzyl ligand. Low-temperature photochemistry allowed for the NMR characterization of an intermediate preceding the hydrogen elimination, identified as the carbene hydride [Mo₂Cp₂(H)(μ-CHPh)(μ-P^tBu₂)(CO)] (**10**), a

product which evolves slowly by H₂ elimination to the benzyldiyne derivative. Analogous dehydrogenation of the methyl ligand in **7** could be accomplished upon moderate heating, to yield the corresponding methylidyne derivative [Mo₂Cp₂(μ-CH)(μ-P^tBu₂)(μ-CO)] (**9**). A complete reaction mechanism accounting for these photochemical reactions was elaborated, based on the reaction intermediates identified experimentally and on extensive DFT calculations. Surprisingly, for both systems the C–H bond activation steps are relatively easy thermal processes occurring with modest activation energies after photochemical ejection of CO, with a rate-determining step involving the formation of agostic carbenes requiring also a strong structural reorganization of the central Mo₂PC rings of these molecules.

Introduction

The use of sterically encumbering ligands has allowed paramount advancements in the kinetic stabilization of otherwise unstable or too reactive transition metal complexes, then providing the opportunity to observe unconventional bonding motifs which typically are translated into new chemical reactivity.¹ A seminal example of this approach was the stabilization of a metal-metal quintuple bond between Cr atoms facilitated by the steric protection provided by bulky terphenyl ligands reported in 2005 by Power and coworkers,² and all the fascinating chemistry around this type of complexes developed afterward.³ Amongst the different groups used for the incorporation of sterically demanding functionalities, P-donor ligands are particularly well suited since they are, in general, readily available and have tunable and predictable electronic and steric properties.⁴ Besides the ubiquitous tertiary phosphanes (PR₃), other bulky organophosphorous ligands with lower coordination numbers at the P atom, such as phosphanyls (–PR₂) or phosphanylidenes (–PR), have also been used for the stabilization of unusual transition metal species, especially in the case of di- or polynuclear metal complexes.^{4b} In this area, our own group has developed a systematic study of the synthesis and reactivity of highly unsaturated binuclear complexes stabilized by phosphanyl bridging ligands.⁵ In particular, we developed selective routes leading to the 30-electron anions [M₂Cp₂(μ-PR₂)(μ-CO)₂][–] (M = Mo, R = Cy, Et, Ph, OEt;⁶ M = W, R = Cy⁷), via two-electron reduction of the corresponding halide-bridged complexes [M₂Cp₂(μ-X)(μ-PCy₂)(CO)₂] (M = Mo, X = Cl; M = W, X = I). In the case of the dimolybdenum systems, we found that the nature of the substituents at the phosphanyl bridge, in

particular their size, was a critical factor in determining the overall stability of these unsaturated species and, in fact, only the relatively bulky PCy₂-bridged complexes were stable enough to be used for further studies on their chemical behavior. Rewardingly, the PCy₂-bridged anions displayed a rich chemistry when confronted with electrophiles, this allowing for the preparation of a range of unsaturated derivatives with different functionalities (i.e. hydride, alkyl or alkoxy-carbyne groups), which in turn also had remarkable chemical behavior.⁵ Our results also revealed that not only the phosphanyl ligand has a strong influence in this chemistry, but also the nature of the metal center (Mo *vs.* W). For instance, the dimolybdenum hydride [Mo₂Cp₂(μ-H)(μ-PCy₂)(CO)₂] displays a structure with terminal carbonyls and a bridging hydride,⁸ while its ditungsten analogue exists in solution as an equilibrium mixture of two isomers having either a terminal or a bridging hydride, although the latter isomer is always dominant.^{7, 9} From all this chemistry it was clear that a subtle balance of steric and electronic effects exerts a strong influence on the chemical reactivity and overall stability of all these unsaturated species. Then, it seemed of interest to test if the use of a bridging phosphanyl group bearing even more sterically demanding substituents could also act as a game changer in terms of chemical reactivity and/or stability of the resulting unsaturated derivatives. In this contribution we give full details of the preparation of the *tert*-butylphosphanyl-bridged 30-electron anion [Mo₂Cp₂(μ-P^tBu₂)(μ-CO)₂]⁻ and some of the neutral derivatives resulting from its reactions with different electrophiles. Our results prove that the presence of a P^tBu₂ ligand indeed has a significant influence on the structure of some of these species, and also on the decarbonylation reactions of the 32-electron alkyl derivatives [Mo₂Cp₂(μ-κ¹:η²-CH₂R)(μ-P^tBu₂)(CO)₂], obtained by reaction of the anion with C-based electrophiles. As it will be seen, these reactions take place now more rapidly and selectively than those for their PCy₂-bridged counterparts to typically form carbyne products following from dehydrogenation of the alkyl bridges. The increased stability provided by the P^tBu₂ ligand to some of the unsaturated species involved in these reactions, such as the 30-electron alkyl [Mo₂Cp₂(μ-κ¹:η²-CH₃)(μ-P^tBu₂)(μ-CO)] or the carbene hydride intermediate [Mo₂Cp₂(H)(μ-CHPh)(μ-P^tBu₂)(CO)], was a key factor allowing us to depict a full reaction pathway accounting for these unusual transformations (μ-CH₂R → μ-CR), also supported by high level DFT calculations which show an excellent match with the experimental results.

Results and Discussion

Synthesis and Structural Characterization of the Chloride Complex 1 and the Unsaturated Anion 2. As mentioned above, a series of unsaturated dimolybdenum anions of formula $[\text{Mo}_2\text{Cp}_2(\mu\text{-PR}_2)(\mu\text{-CO})_2]^-$ have been prepared in our laboratory by reduction of the corresponding chloride complexes $[\text{Mo}_2\text{Cp}_2(\mu\text{-Cl})(\mu\text{-PR}_2)(\text{CO})_2]$, which in turn are prepared from the commercially available reagents $[\text{Mo}_2\text{Cp}_2(\text{CO})_6]$ and ClPR_2 in one step. Fortunately, the same procedure works fine for the preparation of the related P^tBu_2 -bridged complexes. Thus, in a first step a mixture of $[\text{Mo}_2\text{Cp}_2(\text{CO})_6]$ and ClP^tBu_2 is refluxed in xylene for *ca.* 1 h to give a green solution containing the chloride complex $[\text{Mo}_2\text{Cp}_2(\mu\text{-Cl})(\mu\text{-P}^t\text{Bu}_2)(\text{CO})_2]$ (**1**) as major species (Chart 1). Although the bulk of this product could not be properly isolated in a pure form due to its partial decomposition on manipulation, the crude material obtained upon solvent removal from the above reaction mixtures was shown (by IR and NMR) to contain sufficiently pure **1** so as to allow for the selective preparation of the corresponding unsaturated anion. Indeed, two-electron reduction of **1** with reducing agents such as $\text{Li}[\text{BHET}_3]$ or $\text{Na}(\text{Hg})$ in THF takes place rapidly to give red solutions or suspensions, respectively, of the corresponding alkali metal salts of the anion $[\text{Mo}_2\text{Cp}_2(\mu\text{-P}^t\text{Bu}_2)(\mu\text{-CO})_2]^-$ (**2-Li** and **2-Na**) (Chart 1). Not unexpectedly, these anions also are quite air-sensitive species, this preventing us from obtaining them as pure solids. Yet, all available spectroscopic data are indicative of the presence of these salts as major species after reduction, a situation also evidenced by the highly selective reactions of these anions when confronted with different electrophiles (see below).

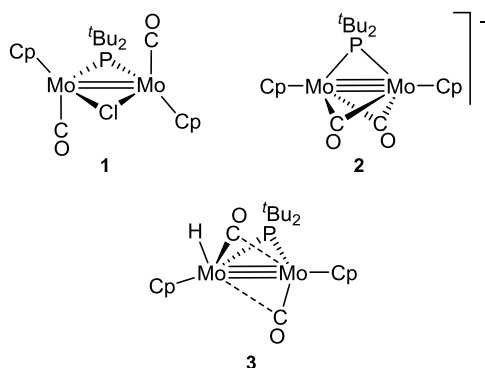


Chart 1

As mentioned above, compound **1** could not be purified in a conventional way, yet we could grow a small crop of X-ray quality crystals for this compound, a situation which proved impossible for related complexes bearing smaller phosphanyl ligands due to rapid decomposition. Its structure in the solid state (Figure 1 and Table 1) is built from two MoCp(CO) fragments arranged in a relative *transoid* disposition and bridged by a chlorine atom and a P^tBu₂ group. Overall the structure resembles that of the hydride-bridged complex [Mo₂Cp₂(μ-H)(μ-PCy₂)(CO)₂], yet some differences are also evident. Firstly, the Mo–Mo bond length of 2.632(1) Å in **1** is nearly 0.1 Å longer than the one measured for the hydride complex (*ca.* 2.53 Å),^{8, 6b, 6a} this being in agreement with the formal reduction of the intermetallic bond order in one unit (from M≡M to M=M) when replacing H (1e-donor) with Cl (3e-donor) at the bridging position.¹⁰ Moreover, the intermetallic separation in **1** is comparable to the ones found for the isoelectronic (32-electron) complexes *trans*-[Mo₂Cp₂(μ-PCy₂)(μ-X)(CO)₂] bearing bridging carbyne (X = CPh, 2.666(1) Å)¹¹ or azavinylidene ligands (X = N=NHPPh, 2.632(1) Å),¹² but shorter than the corresponding value for the phosphanyl-bridged complex [Mo₂Cp₂(μ-PPh₂)₂(CO)₂] (2.70 Å).¹³ Thus it seems that the intermetallic length in this family of 32e complexes correlates with the electronegativity rather than size of the bridgehead atom of the bridging group. Secondly, we note that the central Mo₂PCl ring in **1** is slightly puckered (P-Mo-Mo-Cl *ca.* 171°), in contrast with the flat central Mo₂PH ring observed in [Mo₂Cp₂(μ-H)(μ-PCy₂)(CO)₂], a distortion which is also accompanied by a significant leaning of one CO ligand towards the intermetallic region (Mo1–Mo2–C2 = 76.3(3)°). This asymmetry is not transmitted to the coordination of the bridging ligands, these displaying an almost perfectly symmetric coordination, with the Mo–Cl bond lengths (*av.* 2.50 Å) being comparable to those measured for related complexes such as [Mo₂(Cp^R)₂(μ-Cl)(μ-PPh₂)₂] (*ca.* 2.52 Å; Cp^R = η⁵-C₅Me₄Et)¹⁴ or [Mo₂Cp₂(μ-Cl)(μ-PPh₂)(μ-SMe)₂] (*ca.* 2.53 Å).¹⁵

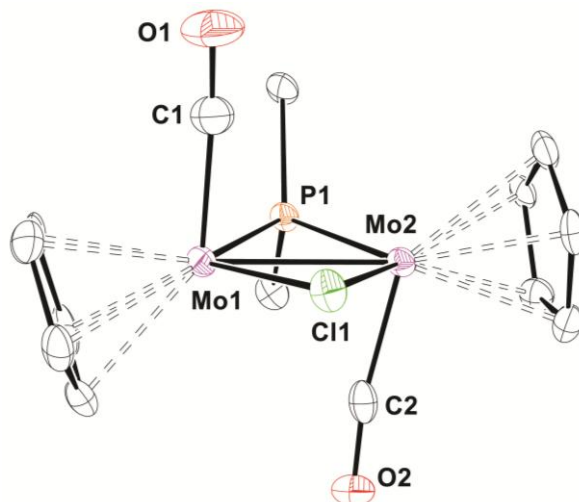


Figure 1. ORTEP diagram (30 % probability) of compound **1**, with H atoms and ^tBu groups (except C¹ atoms) omitted for clarity.

Table 1. Selected Bond Lengths (Å) and Angles (°) for Compound **1**.

Mo1–Mo2	2.632(1)	Mo1–P–Mo2	66.07(7)
Mo1–P	2.428(3)	Mo1–C11–Mo2	63.64(6)
Mo2–P	2.400(3)	Mo1–Mo2–C2	76.3(3)
Mo1–C11	2.505(3)	Mo2–Mo1–C1	87.9(4)
Mo2–C11	2.487(3)	P–Mo1–C1	89.5(4)
Mo1–C1	1.946(14)	P–Mo2–C2	90.4(3)
Mo2–C2	1.920(13)	Mo1–C1–O1	171.8(13)
		Mo2–C2–O2	170.7(9)

Spectroscopic data in solution for **1** (Table 2 and Experimental Section) are consistent with its solid-state structure and comparable to those of the family of complexes $[\text{Mo}_2\text{Cp}_2(\mu\text{-Cl})(\mu\text{-PR}_2)(\text{CO})_2]$ bearing different phosphanyl bridges.^{6b} In particular, the retention of a *transoid* $\text{Mo}_2(\text{CO})_2$ oscillator is clearly denoted by the IR spectrum, which displays two C–O stretching bands with weak and strong relative intensities in order of decreasing frequency.¹⁶ However, there are two significant differences in the IR spectrum of **1** when compared to those of the related chloride complexes having less sterically demanding phosphanyl ligands. In first place, the relative intensity of the most energetic band (symmetric C–O stretching, 1891 cm^{-1}) is significantly higher for **1** and, secondly, the separation between the two bands is also bigger [42 cm^{-1} vs. 36 (PCy_2 and PEt_2), 34 (PPh_2) or 23 ($\text{P}(\text{OEt}_2)$)].^{6b} These differences can be explained by recalling the significant distortion of some 10° away from the ideal *transoid* arrangement with

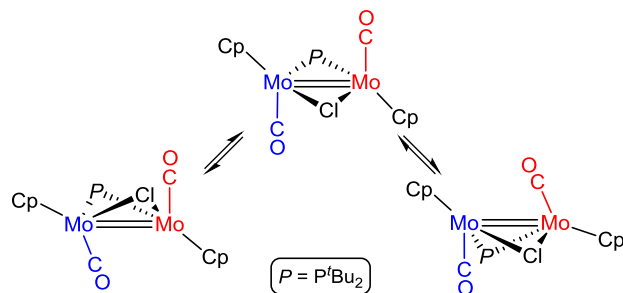
antiparallel carbonyls observed in the solid-state structure of **1** (Figure 1). We must note that similar IR patterns were observed for the stannyl-bridged complexes $[\text{M}_2\text{Cp}_2(\mu\text{-PCy}_2)(\mu\text{-SnPh}_3)(\text{CO})_2]$ ($\text{M} = \text{Mo},^{17} \text{W}^9$), which also display significantly distorted *transoid* $\text{M}_2(\text{CO})_2$ fragments in their solid state structures, supposedly retained in solution.

Table 2. Selected IR^a and NMR^b spectroscopic data for new compounds.

Compound	$\nu(\text{CO})$	$\delta(\mu\text{-P})$	$\delta(\mu\text{-C}) [J_{\text{CP}}]$
$[\text{Mo}_2\text{Cp}_2(\mu\text{-Cl})(\mu\text{-P}^t\text{Bu}_2)(\text{CO})_2]$ (1)	1889 (m), 1846 (vs) ^c	215.9	
$\text{Li}[\text{Mo}_2\text{Cp}_2(\mu\text{-P}^t\text{Bu}_2)(\mu\text{-CO})_2]$ (2-Li)	1656 (w), 1589 (m, sh), 1562 (vs) ^c	240.3 ^d	
$\text{Na}[\text{Mo}_2\text{Cp}_2(\mu\text{-P}^t\text{Bu}_2)(\mu\text{-CO})_2]$ (2-Na)	1652 (w), 1588 (vs) ^c	– ^e	
$[\text{Mo}_2\text{Cp}_2(\text{H})(\mu\text{-P}^t\text{Bu}_2)(\text{CO})_2]$ (3)	1825 (s), 1794 (vs) ^f	288.6 ^{g,h}	
$[\text{Mo}_2\text{Cp}_2(\mu\text{-}\kappa^1\text{:}\eta^2\text{-CH}_3)(\mu\text{-P}^t\text{Bu}_2)(\text{CO})_2]$ (4a)	1883 (m), 1835 (vs) ^f	209.4 ⁱ	–42.3 [3] ^j
$[\text{Mo}_2\text{Cp}_2(\mu\text{-}\kappa^1\text{:}\eta^2\text{-CH}_2\text{Ph})(\mu\text{-P}^t\text{Bu}_2)(\text{CO})_2]$ (4b)	1901 (m), 1843 (vs) ^f	204.6 ⁱ	–3.5 [0] ^j
$[\text{Mo}_2\text{Cp}_2(\mu\text{-COMe})(\mu\text{-P}^t\text{Bu}_2)(\mu\text{-CO})]$ (5)	1673 (s)	259.0 ⁱ	353.6 [14] ^k
$[\text{Mo}_2\text{Cp}_2(\mu\text{-P}^t\text{Bu}_2)(\mu\text{-SnPh}_3)(\text{CO})_2]$ (6)	1866 (m), 1796 (vs)	297.4 ^{i,k}	
$[\text{Mo}_2\text{Cp}_2(\mu\text{-}\kappa^1\text{:}\eta^2\text{-CH}_3)(\mu\text{-P}^t\text{Bu}_2)(\mu\text{-CO})]$ (7)	1715 (s) ^f	266.2	41.3 [6] ^{g,l}
$[\text{Mo}_2\text{Cp}_2(\mu\text{-CH})(\mu\text{-P}^t\text{Bu}_2)(\mu\text{-CO})]$ (8)	1726 (s) ^f	258.6	383.1 [15]
$[\text{Mo}_2\text{Cp}_2(\mu\text{-CPh})(\mu\text{-P}^t\text{Bu}_2)(\mu\text{-CO})]$ (9)	1686 (s)	265.2 ^k	385.9 [14] ^k
$[\text{Mo}_2\text{Cp}_2(\text{H})(\mu\text{-CHPh})(\mu\text{-P}^t\text{Bu}_2)(\text{CO})]$ (10)	1783 (s) ^f	287.8 ^m	131.3 ^m

^a Recorded in dichloromethane solution, unless otherwise stated, with C–O stretching bands ($\nu(\text{CO})$) in cm^{-1} . ^b Recorded in C_6D_6 solution at 400.13 (^1H), 162.12 ($^{31}\text{P}\{^1\text{H}\}$) or 100.63 MHz ($^{13}\text{C}\{^1\text{H}\}$) and 298 K unless otherwise stated, with coupling constants (J) given in Hertz. ^c Recorded in THF. ^d Recorded at 121.49 MHz in THF- d_8 . ^e The low solubility of this salt prevented us from collecting its NMR data. ^f Recorded in petroleum ether. ^g Recorded in toluene- d_8 . ^h The ^1H NMR hydride resonance in toluene- d_8 appeared at –2.48 ppm (d, $J_{\text{HP}} = 31$ Hz). ⁱ Recorded at 121.49 MHz. ^j Recorded at 75.47 MHz. ^k Recorded in CD_2Cl_2 . ^l Recorded at 223 K. ^m Recorded in CD_2Cl_2 at 253 K.

As for the NMR data, compound **1** displays a single ^{31}P NMR resonance (215.9 ppm) some 60 ppm above the one measured for the related PCy_2 -bridged complex (155.9 ppm), a difference also found when comparing related pairs of complexes bearing these phosphanyl bridges (cf. $[\text{Mo}_2\text{Cp}_2(\mu\text{-H})(\mu\text{-PR}_2)(\text{CO})_4]$, $\text{R} = \text{Cy}$ (219 ppm),¹⁸ ^tBu (268 ppm)¹⁹). The ^1H NMR spectrum displays just one set of signals for the Cp and ^tBu groups, which is inconsistent with the asymmetric structure denoted by the IR and X-ray data. This suggest the existence of a fast (on the NMR timescale) concerted exchange of the CO and Cp environments in solution, also present in the mentioned stannyl-bridged complexes $[\text{M}_2\text{Cp}_2(\mu\text{-PCy}_2)(\mu\text{-SnPh}_3)(\text{CO})_2]$,^{17,9} likely occurring in this case through an intermediate structure displaying a C_2 -symmetry and related to that of the hydride-bridged complex $[\text{Mo}_2\text{Cp}_2(\mu\text{-H})(\mu\text{-PR}_2)(\text{CO})_2]$ (Scheme 1).



Scheme 1

Spectroscopic data for the Li^+ and Na^+ salts of the anion **2** (Table 2 and Experimental Section) are in excellent agreement with those of the large family of unsaturated anions having various bridging phosphanyl ligands prepared in our laboratory,^{6b, 7} therefore a similar structure is to be assumed for all these carbonyl-bridged complexes (Chart 1). The IR spectra of anion **2** is quite sensitive to the nature of the counter cation present, which is indicative of the existence of ion-pairing effects in solution, a quite common situation for transition metal carbonylates²⁰ which we studied in detail for the PCy_2 -bridged anion,^{6b} then a detailed discussion of these data is unnecessary here. We will only note that the two low-frequency bands expected for a complex with two bridging CO ligands defining an angle close to 120° were observed only for **2-Li**, while the spectra of **2-Na** displays just one stretching band, likely occurring due to overlap of the corresponding stretches. In addition, the spectra of both salts display additional weak high-frequency bands (1656 (**2-Li**) and 1652 (**2-Na**) cm^{-1}) due to the presence in solution of molecules of the anion bearing $\text{O}\cdots\text{M}$ ($\text{M} = \text{Li}, \text{Na}$) interactions located exclusively at one of the two CO ligands. This type of ion pairs were observed only for the Li^+ salt of the anion $[\text{Mo}_2\text{Cp}_2(\mu\text{-PCy}_2)(\mu\text{-CO})_2]^-$, but was totally absent for the corresponding Na^+ salt or for any salt of the analogous ditungsten anion. All this suggests that the presence of a bulkier phosphanyl ligand in **2** favors somewhat the formation of ion pairs involving only one of the bridging CO ligands. Finally, we must note that the presence of all these associative phenomena denoted by the IR data is not reflected in the NMR spectra of **2**, which otherwise display averaged ^{31}P and ^1H NMR resonances consistent with the presence of a highly symmetric anion with equivalent Cp and ^tBu groups.

Synthesis and Structural Characterization of the Hydride 3. The unsaturated anion **2** can be easily protonated even with mild acids such as NH_4PF_6 to give the corresponding unsaturated

hydride $[\text{Mo}_2\text{Cp}_2(\text{H})(\mu\text{-P}^t\text{Bu}_2)(\text{CO})_2]$ (**3**) in high yield (*ca.* 85% from $[\text{Mo}_2\text{Cp}_2(\text{CO})_6]$) (Chart 1). This compound can be conveniently purified by column chromatography and remains stable for long periods of time when stored at low temperature under argon. Quite unexpectedly for an unsaturated compound, a terminal disposition of the hydride ligand is found in solution and in the solid state for **3** (*vide infra*), while the carbonyl ligands display linear semibridging coordination. As mentioned before, this situation is in stark contrast with the structure of the related PCy₂-bridged hydride $[\text{Mo}_2\text{Cp}_2(\mu\text{-H})(\mu\text{-PCy}_2)(\text{CO})_2]$, a complex displaying instead a more conventional bridging coordination of the hydride ligand and terminal carbonyls. The terminal disposition of the hydride in **3** is not completely unprecedented since the related ditungsten hydride $[\text{W}_2\text{Cp}_2(\text{H})(\mu\text{-PCy}_2)(\text{CO})_2]$ exists in solution as an equilibrium mixture of isomers with either a terminal or a bridging hydride, although the latter isomer is dominant at all temperatures, so that the structural information about the terminal isomer is yet quite limited.⁹ Finally, we must note that the hydride **3** can be converted selectively back into the corresponding anion by reaction with different reducing agents (i.e. Na(Hg), Li[BHET₃], etc.), then being a quite convenient source of the unsaturated anion itself.

The molecular structure of **3** in the crystal (Figure 2 and Table 3) confirms the terminal coordination of the hydride ligand at the Mo1 atom (Mo1–H1 1.69(3) Å; Mo2–Mo1–H1 103(1)°), with the two MoCp fragments being bridged by a symmetrically coordinated phosphanyl ligand and by two semibridging carbonyls, a structure resembling that of the isoelectronic cation $[\text{Mo}_2\text{Cp}_2(\text{H})(\mu\text{-PCy}_2)_2(\text{CO})]^+$ (Mo–H 1.65(9) Å; Mo–Mo–H 103(3)°).²¹ The short intermetallic separation in **3**, 2.5145(3) Å, is consistent with the formulation of a metal-metal triple bond for this 30-electron complex, being *ca.* 0.75 Å shorter than that of the corresponding saturated hydride $[\text{Mo}_2\text{Cp}_2(\mu\text{-H})(\mu\text{-P}^t\text{Bu}_2)(\text{CO})_4]$,¹⁹ in fact resulting almost identical to those measured for isoelectronic hydrides such as the above mentioned cation (2.534(2) Å)²¹ or the PCy₂-bridged analogue of **3** (2.528(2) Å),^{6b, 8} even if the latter displays a bridging hydride ligand. The two CO ligands display linear semibridging coordination of type II, according to the nomenclature proposed by Crabtree and Lavin for these ligands,²² which is a common feature found in binuclear carbonyl complexes displaying intermetallic triple bonds.⁵ However, the strength of this interaction is markedly different in each case, as indicated by the corresponding M···C distance, significantly shorter for the carbonyl attached to the H-bearing

Mo atom (2.338(2) vs. 2.526(2) Å), a structural effect likely related to the higher coordination number of this metal site.

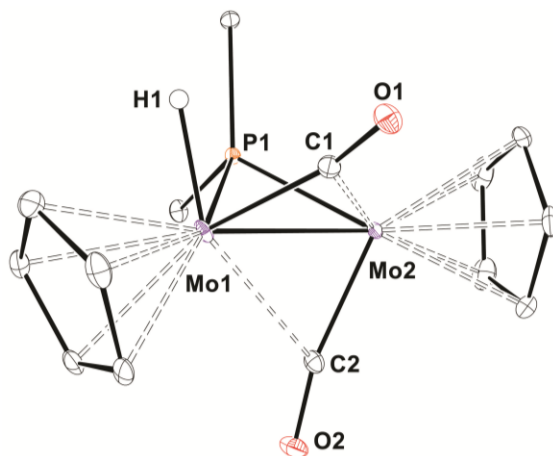


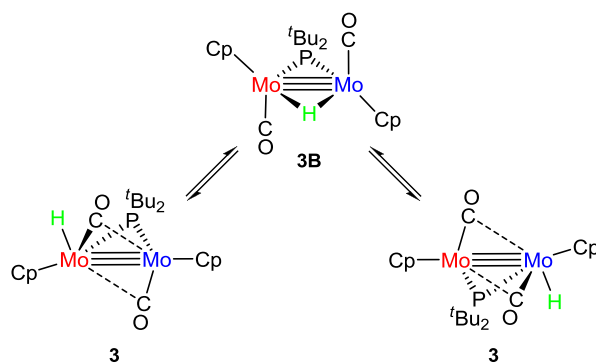
Figure 2. ORTEP diagram (30 % probability) of compound **3**, with H atoms (except H1) and ^tBu groups (except C¹ atoms) omitted for clarity.

Table 3. Selected Bond Lengths (Å) and Angles (°) for Compound **3**.

Mo1–Mo2	2.5145(3)	Mo1–P–Mo2	62.725(14)
Mo1–P	2.4292(6)	P–Mo1–H1	73.9(11)
Mo2–P	2.4019(5)	C1–Mo1–H1	72.4(11)
Mo1–H	1.69(3)	Mo2–Mo1–H1	102.6(11)
Mo1–C1	1.984(2)	Mo1–C1–O1	161.7(2)
Mo1···C2	2.526(2)	Mo1–C2–O2	167.6(2)
Mo2–C2	1.925(2)	Mo1–Mo2–C2	67.87(6)
Mo2–C1	2.338(2)	Mo2–Mo1–C1	61.29(6)

Spectroscopic data for compound **3** (Table 2 and Experimental Section) are essentially compatible with its solid-state structure, although they are also indicative of fluxional behavior in solution. Thus, the IR spectrum displays two strong C–O stretching bands (1813 (s) and 1778 (vs) cm⁻¹) with relative intensities in agreement with the presence of *transoid* carbonyl ligands defining relative angles well below 180°. ¹⁶ The low frequency of these bands, when compared to those of [Mo₂Cp₂(μ-H)(μ-PCy₂)(CO)₂] (1858 and 1829 cm⁻¹), support the retention in solution of the semibridging coordination found for the carbonyls in the solid state, also indicated by the high chemical shift of the corresponding ¹³C NMR resonances (δ_C = 271 and 261 ppm at 173 K; cf. 248 ppm in the PCy₂-bridged compound). ^{6b} The ³¹P NMR spectrum of **3** displays a

temperature-independent and highly deshielded resonance at 290 ppm, a chemical shift close to the values found for related compounds bearing P^tBu₂ ligands bridging metal-metal triple bonds (cf. 280 ppm for [Mo₂Cp₂(μ-P^tBu₂)(μ-PCyH)(μ-CO)]).¹⁸ In contrast, the ¹H and ¹³C NMR spectra of **3** at room temperature are inconsistent with the asymmetric structure found in the crystal, since they reflect the presence of an apparent C₂-symmetry axis that renders equivalent Cp, CO and ^tBu pairs of groups (see the Supporting Information). However, on lowering the temperature (173 K) all these signals eventually split into well-resolved pairs of resonances for each of these groups, now in agreement with the static solid-state structure, which is devoid of any symmetry. We must note that a simple exchange of the hydride ligand between the two Mo centers must be discarded as the fluxional process in **3** on the basis of the equivalence of the CO and ^tBu groups in the fast exchange regime. Instead, the exchange of the hydride ligand likely takes place through a hydride-bridged isomer **3B** (not observed) with a structure identical to that of the related PCy₂ complex (Scheme 2), actually a structure computed to be only *ca.* 1.7 kJ·mol⁻¹ above that of the terminal isomer in the potential energy surface of the system (see below). This fluxional process does not affect the ¹H NMR resonance of the hydride ligand, which appears as a poorly shielded doublet (δ = -2.54 ppm, J_{HP} = 31 Hz), being almost 5 ppm above that measured for the H-bridging ligand in the PCy₂ compound (δ_H = -6.94 ppm), while remaining close to that found for the isoelectronic cation [Mo₂Cp₂(H)(μ-PCy₂)₂(CO)]⁺ (δ_H = -1.60 ppm).²¹



Scheme 2

DFT Calculations of Compound 3. The theoretical description of M–M bonding interactions in organometallic complexes is a topic of current interest,²³ particularly in the case of multiply bonded compounds which typically bear bridging ligands that further complicate the description

of the M–M interactions in simple terms. In particular, the nature of M–M bonding in complexes with bridging hydrides or alkyls is the subject of controversy due to the presence of M–H–M tricentric interactions. Thus, Green and col. introduced some time ago the “half-arrow” notation,²⁴ a convention which assumes that these bridging ligands act effectively as three-electron donors, this resulting in a reduction in one unit of the M–M bond order (BO) assigned to these complexes, when compared to the BO resulting from the application of the 18-electron rule (i.e. M=M vs. M≡M for [Mo₂Cp₂(μ-H)(μ-PR₂)(CO)₂]). This interpretation is sustained by early calculations on electron-deficient complexes of the type M₂(μ-H)_x (x ≥ 2)²⁵ or those on the formate complex [Mo₂Cp₂(μ-H)(μ-PH₂)(μ-O₂CH)₂],²⁶ all leading to the conclusion that no direct M–M bonds were present in these complexes. Although neglecting the existence of direct M–M bonding character in the M–H–M tricentric interactions seems reasonable for complexes with long intermetallic separations we believe that, for very short separations, significant direct M–M bonding character is to be retained in these interactions. In agreement with this view, our DFT calculations on the unsaturated hydride [Mo₂Cp₂(μ-H)(μ-PCy₂)(CO)₂] supported the presence of a M–M triple bond in such H-bridged complex, with the intermetallic bonding following from three components: one tricentric Mo₂H and two bicentric Mo₂ (σ and π) bonding interactions.⁸ The Atoms-In-Molecules (AIM)²⁷ analysis of this complex (and other bond indicators) also supported the formulation of a metal–metal triple bond, because the electron density (ρ_{MM} = 0.582 eÅ⁻³) accumulated at the corresponding M–M bond critical point (bcp) was comparable to those calculated at the same level for triply bonded complexes without bridging ligands (i.e. [Mo₂Cp₂(CO)₄]), or for the parent anion [Mo₂Cp₂(μ-PCy₂)(μ-CO)₂]⁻ (0.615 eÅ⁻³).²⁸

In this context, we reasoned that the DFT calculation of the geometry and electronic structure of compound **3** could provide relevant information about the metal-metal bonding interactions in this type of unsaturated hydrides and the unexpected preference for the terminal coordination of the hydride ligand. For comparison, we have also computed the hypothetical H-bridged isomer [Mo₂Cp₂(μ-H)(μ-P^tBu₂)(CO)₂] (**3B**). Geometry optimization of both isomers using the B3LYP functional allowed the localization of the corresponding minima in the Potential Energy Surface (see SI). Quite surprisingly, at this level of computation the H-bridged structure **3B** was predicted to have a Gibbs free energy 2.3 kJ·mol⁻¹ lower than the terminal isomer **3**, a situation in clear contradiction with the exclusive observation of the latter both in solution and in the solid

state. However, introduction of solvent effects (toluene) via the Polarizable Continuum Model (PCM),²⁹ or inclusion of Grimme's dispersion correction accounting for van der Waals dispersive forces (B3LYP-D2),³⁰ reversed the energetic ordering, with the terminal isomer **3** now being 0.3 (PCM) or 1.7 (B3LYP-D2) kJ·mol⁻¹ more stable than the H-bridged isomer **3B**. From all this we conclude that the energetic differences between isomers **3** and **3B** are very small in spite of their very different structures, which is not surprising since analogous isomers coexist in solution for the related ditungsten complex [W₂Cp₂(H)(μ-PCy₂)(CO)₂], as noted above.⁹ In any case, the following discussion will only use the B3LYP-D2 derived data which, as judging from the energetic differences, seems to give a more adequate description of the systems under study.

The optimized geometries of isomers **3** and **3B** (Figure 3 and Table 4) are in good agreement with the corresponding reference experimental data. In particular, the computed structure for **3** is essentially identical to the one determined crystallographically for this complex, then deserving no additional comments. In the case of the H-bridged isomer **3B** the main difference with the solid-state structure of [Mo₂Cp₂(μ-H)(μ-PCy₂)(CO)₂],³¹ lies in the slightly puckered central Mo₂PH ring (P–Mo–Mo–H = 164.7°), which is accompanied by the leaning of one CO ligand towards the intermetallic vector (Mo–Mo–C = 76.3 and 91.5°). This kind of distortion was not observed for the PCy₂ complex (nor predicted for **3B** at the B3LYP level!), but it is similar (if less pronounced) to the one found for the chloride complex **1**, and surely related to the presence of the bulky P^tBu₂ ligand, as noted already.

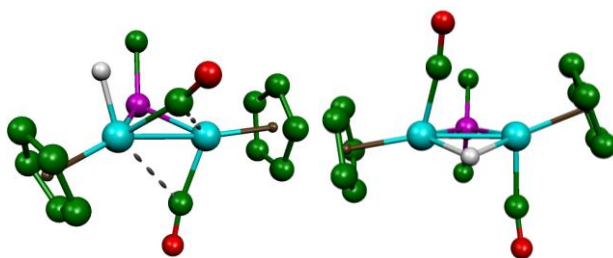


Figure 3. Optimized structures (B3LYP-D2) for compounds **3** (left) and **3B** (right), with H atoms (except hydride ligands) and ^tBu groups (except C¹ atoms) omitted for clarity.

Table 4. Selected Geometric Parameters of the Optimized and Experimental Structures of Isomers **3** and **3B**.

	3	X-ray	3B	Xray ^a
Mo1–Mo2	2.526	2.5145(3)	2.550	2.528(2)
Mo1–P	2.440	2.4292(6)	2.433	2.386(3)
Mo2–P	2.398	2.4019(5)	2.414	2.383(3)
Mo1–H	1.687	1.69(3)	1.885	1.84(8)
Mo2–H	–	–	1.886	1.88(10)
Mo1–C1	2.001	1.984(2)	1.950	1.92(1)
Mo1–C2	2.661	2.526(2)	–	–
Mo2–C2	1.944	1.925(2)	1.943	1.90(1)
Mo2–C1	2.376	2.338(2)	–	–
Mo1–P–Mo2	62.9	62.725(14)	63.5	64.0(1)
Mo1–H–Mo2	–	–	85.1	85(4)
P–Mo1–H1	76.4	73.9(11)	104.1	
C1–Mo1–H1	75.2	92.67(8)	79.0	
Mo2–Mo1–H1	104.8	102.6(11)		
P–Mo1–Mo2–H1			164.7	179

^a Data for [Mo₂Cp₂(μ-H)(μ-PCy₂)(CO)₂] taken from reference ³¹.

The frontier occupied molecular orbitals of isomers **3** (Figure 4) and **3B** (see Table S6 in the Supporting Information) can be related to those previously computed by us for the anion [Mo₂Cp₂(μ-PCy₂)(μ-CO)₂][–] and the hydride [Mo₂Cp₂(μ-H)(μ-PCy₂)(CO)₂],^{28, 8} respectively. In the terminal isomer **3**, the HOMO represents one of the σ bonding interactions of the semibridging carbonyl with strongest binding to the second metal, while the following three orbitals are those accounting for the expected metal-metal triple bond with one σ (HOMO–3) and two δ type components (HOMO–2 and HOMO–1), the latter ones being mixed with π-backbonding with the CO ligands, then reducing somewhat the direct M–M character of these interactions. As for the H-bridged isomer **3B**, the metal-metal bonding is built from two bicentric Mo₂ components (σ and π) and a tricentric Mo₂H interaction, exactly in the same way as found for the PCy₂ analogue. Thus it can be concluded that the above mentioned distortion of the central PMo₂H skeleton in **3B** has no significant effects on the intermetallic orbital interactions. The AIM analysis (Table 5) also provides additional support to the presence of intermetallic triple bonds in these isomers, this being evidenced by the relatively high values of the electron density at the corresponding intermetallic bcp's [0.573 (**3**) and 0.568 (**3B**) eÅ^{–3}], approaching the

values found for isoelectronic species of the type $[\text{Mo}_2\text{Cp}_2(\mu\text{-PR}_2)(\mu\text{-X})(\mu\text{-CO})]$ ($X = \text{PR}_2, \text{COMe}$) (ca. $0.6 \text{ e}\text{\AA}^{-3}$), and being essentially identical to the value of 0.576 \AA computed at the same level for $[\text{Mo}_2\text{Cp}_2(\text{CO})_4]$.²⁸ It is also evident that the exchange of the hydride ligand from bridging to terminal position only increases quite modestly the corresponding electron density at the intermetallic bcp, a situation which gives additional support to our view of the retention of significant direct M–M bonding character in the tricentric Mo_2H interaction at the bridged isomers.

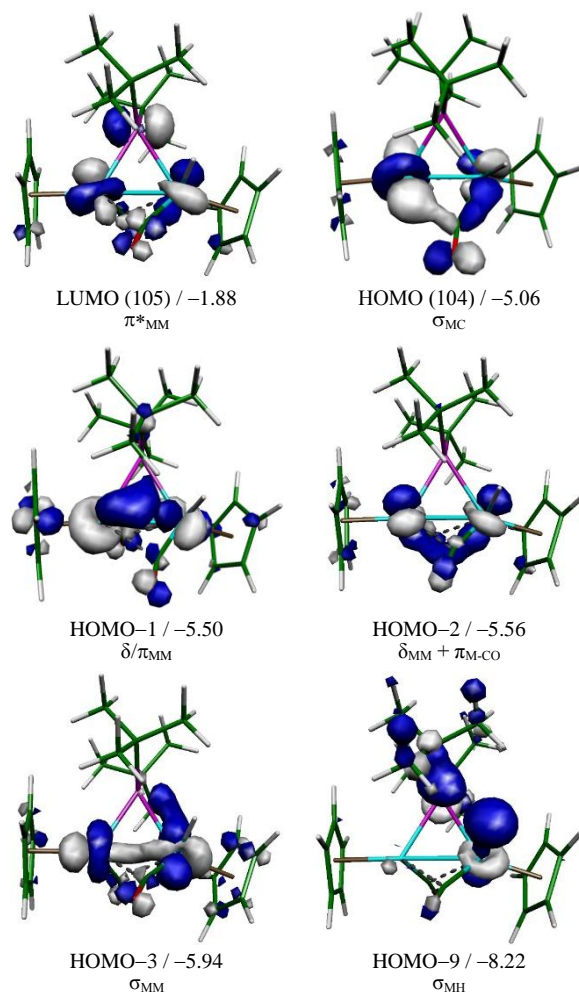


Figure 4. Selected molecular orbitals for compound **3** (B3LYP-D2), with energy (eV) and dominant character shown below.

Table 5. Topological Properties of the Electron Density at the Bond Critical Points for Isomers **3** and **3B**.^a

Bond	3			3B		
	ρ	$\nabla^2\rho$	MBI ^b	ρ	$\nabla^2\rho$	MBI ^b
Mo–Mo	0.573	2.321	1.111	0.568	2.015	1.180
Mo1–P	0.527	3.457	0.815	0.554	3.273	0.865
Mo2–P	0.570	3.321	0.885	0.529	3.400	0.881
Mo1–H	0.784	2.440	0.856	0.485	3.753	0.424
Mo2–H	–	–	–	0.486	3.749	0.475
Mo1–C1	0.850	8.135	1.015	0.934	10.487	1.134
Mo2–C2	0.959	9.673	1.136	0.962	10.009	1.162
Mo1–C2	–	–	0.250	–	–	–
Mo2–C1	0.417	4.478	0.394	–	–	–

^a Values of the electron density at the bond critical points (ρ) are given in $\text{e}\text{\AA}^{-3}$; values of the Laplacian of ρ at these points ($\nabla^2\rho$) are given in $\text{e}\text{\AA}^{-5}$. ^b Mayer Bond Index for the corresponding bond.

Reactions of the Unsaturated Anion 2 with Group 14 Electrophiles. Our previous work on the PCy₂-bridged anions $[\text{M}_2\text{Cp}_2(\mu\text{-PCy}_2)(\mu\text{-CO})_2]^-$ (M = Mo, W) proved that these systems display two competitive nucleophilic sites placed at the dimetallic center and at the oxygen atoms of the bridging carbonyls, with this latter position being slightly more favored in the case of the ditungsten compound. When confronted with hydrocarbon halides, however, it was evident that a subtle balance between the properties of the electrophile and those of the anion (metal center, counterion, etc.) would influence the selectivity of these reactions, which could yield up to four possible types of products: i) halide-bridged $[\text{M}_2\text{Cp}_2(\mu\text{-X})(\mu\text{-PCy}_2)(\text{CO})_2]$, ii) hydrocarbyl-bridged $[\text{M}_2\text{Cp}_2(\mu\text{-R})(\mu\text{-PCy}_2)(\text{CO})_2]$, iii) alkoxy-carbyne-bridged $[\text{M}_2\text{Cp}_2(\mu\text{-COR})(\mu\text{-PCy}_2)(\mu\text{-CO})]$ or iv) the iodoxy-carbyne-bridged $[\text{M}_2\text{Cp}_2(\mu\text{-COI})(\mu\text{-PCy}_2)(\mu\text{-CO})]$ derivatives.⁶⁻⁷

With these precedents in mind, we tested a selected number of reactions of the unsaturated anion **2** with different electrophilic reagents. Addition of MeI or PhCH₂Cl to freshly prepared suspensions of **2-Na** led to a progressive solubilization over the course of 2 and 8 h, respectively, to give solutions containing the corresponding alkyl-bridged complexes $[\text{Mo}_2\text{Cp}_2(\mu\text{-}\kappa^1\text{:}\eta^2\text{-CH}_2\text{R})(\mu\text{-P}^t\text{Bu}_2)(\text{CO})_2]$ (R = H (**4a**), Ph (**4b**)) (Chart 2) as major products, along with traces of the corresponding halide complexes $[\text{Mo}_2\text{Cp}_2(\mu\text{-X})(\mu\text{-P}^t\text{Bu}_2)(\text{CO})_2]$. In the reaction with MeI, we also observed the formation of small amounts of the methoxy-carbyne complex $[\text{Mo}_2\text{Cp}_2(\mu\text{-}$

COMe)(μ -P^tBu₂)(μ -CO)] (**5**) (Chart 2), a product following from the competitive binding of the electrophile at the O atom of one of the CO ligands of the parent anion. Keeping in mind that for the PCy₂-bridged anion this type of product was only formed when using stronger methylating reagents (Me₂SO₄ or Me₃OBF₄), it can be concluded that the presence of a more sterically encumbering phosphanyl ligand in **2** enhances somewhat the reactivity at the O position, possibly due to the increased difficulties to access the dimetal center. However, the outcome of the benzyl chloride reaction is essentially identical to the one of the PCy₂-bridged anion, this denoting that steric effects only cannot account for the observed differences. The reaction of **2-Na** with ClSnPh₃ also takes place with incorporation of the SnPh₃⁺ electrophile at the intermetallic position, then leading to the formation of the unsaturated cluster [Mo₂Cp₂(μ -P^tBu₂)(μ -SnPh₃)(CO)₂] (**6**) in a selective manner (Chart 2), a process also observed for the related dimolybdenum and ditungsten PCy₂-bridged anions. Once more, it is evidenced here the strong preference of these unsaturated systems to force an unconventional bridging coordination of the tin fragment, which otherwise tends to adopt typically a terminal coordination. In fact, besides our complexes we can only quote two other families of organometallic compounds bearing bridging SnR₃ moieties, the manganese complexes [Mn₂{ μ -SnR₂OP(OEt₂)}(CO)₆L] (R = Bu, Ph; L = CO, tertiary phosphine),³² and the germanium cluster [K(2,2,2-crypt)][Ge₉(μ -SnPh₃)] (2,2,2-crypt = C₁₈H₃₆N₂O₆).³³

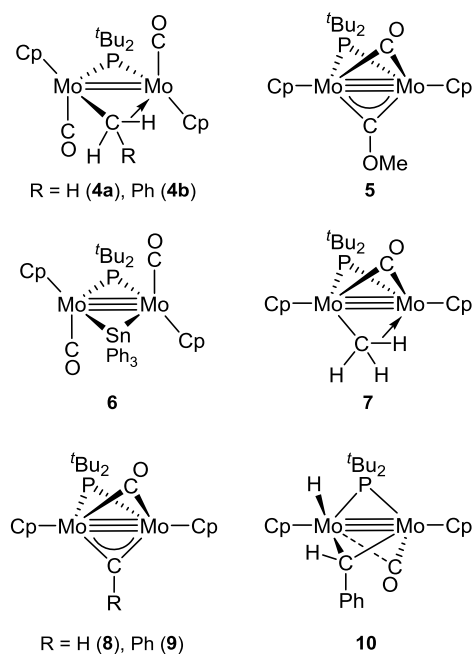


Chart 2

Solution Structure of the Agostic Alkyl Complexes 4. The available spectroscopic data for the alkyl complexes **4a,b** (Table 2 and Experimental Section) draw a clear relationship with the corresponding PCy₂-bridged analogues [M₂Cp₂(μ-κ¹:η²-CH₂R)(μ-PCy₂)(CO)₂] (M = Mo, W), a family of compounds which have been extensively characterized through X-ray diffraction, DFT studies and spectroscopic methods.^{8, 34} Then, a detailed analysis is not required here, and a similar structure is proposed for the new complexes **4a,b**, with a three-electron formal contribution of the bridging alkyl groups to the dimetal center due to the presence of measurable C–H···M agostic interactions. In agreement with this, the ³¹P resonances of these compounds appear around 207 ppm, remaining close to the value of the 32-electron chloride complex **1** (215 ppm), and being significantly lower than the reference figures for 30-electron complexes such as the hydride **3** (290 ppm) or the bis(phosphanyl) complex [Mo₂Cp₂(μ-P^tBu₂)(μ-PCyH)(μ-CO)] (280 ppm).¹⁸ The room temperature ¹H and ¹³C NMR spectra are, however, inconsistent with the static structures depicted in Chart 2 in which the alkyl groups interact via σ coordination to one metal and through the α agostic interaction with the second Mo atom. Thus, in both cases single resonances for the pairs of Cp and CO ligands were observed, this suggesting the presence of an apparent C₂-symmetry axis relating these groups. In the case of **4a** this is also accompanied by the presence of just one ¹H NMR resonance for the three hydrogen atoms of the Me group (−0.74 ppm), while the benzyl derivative **4b** already displays separated signals for the coordinated (−1.94 ppm) and uncoordinated protons (2.59 ppm). These observations suggest the operation of fast fluxional processes in both complexes (not studied) involving rapid exchange of the environment of the H atoms within the Me group (for **4a**) or a 180° rotation of the benzyl group around the C–M vector (for **4b**), these resulting identical to those studied in great detail for the related PCy₂-bridged complexes.⁸ Finally, the IR spectra of both compounds also display C–O stretching bands with the relative intensities being indicative of the presence of a significant distortion from the ideal *transoid* disposition of the Mo₂(CO)₂ oscillator, as already discussed for the chloride complex **1**.

Structural Characterization of the Stannyl Derivative 6. The structure of complex **6** (Figure 5 and Table 6) was determined by an X-ray diffraction analysis, and its structure does not differ substantially from those of the related PCy₂-bridged complexes [M₂Cp₂(μ-PCy₂)(μ-

SnPh₃)(CO)₂] (M = Mo, W) reported previously by us,^{17,9} therefore only brief comments will be included here. The intermetallic bond length in **6** (2.5907(4) Å) is consistent with the formulation of a M–M triple bond, although it is some 0.08 Å longer than the one measured in the hydride **3**, yet comparable to that found for the above mentioned stannyl compounds (*ca.* 2.57 Å).^{9, 17} The central PMo₂Sn ring in **6** is puckered in an extent comparable to the related PCy₂-bridged complex (PMo₂Sn *ca.* 158°), and even more puckered than the corresponding PMo₂Cl ring in **1** (158° *vs.* 171°), thus supporting our view that this structural distortion has a steric origin. In consonance with it, the carbonyl ligands display a stronger deviation from the ideal antiparallel disposition, with one leaning towards the intermetallic vector (Mo2–Mo1–C1 68.9(1)°) so as to be classified as a linear semibridging group (Mo–C1 = 1.923(3) and 2.612(3) Å). This is accompanied by an asymmetric positioning of the SnPh₃ ligand ($\Delta d_{\text{MoSn}} = 0.12$ Å), which is even more pronounced than the ones observed in the PCy₂-bridged analogues ($\Delta d = 0.01$ (Mo₂)¹⁷ and 0.06 Å (W₂)⁹).

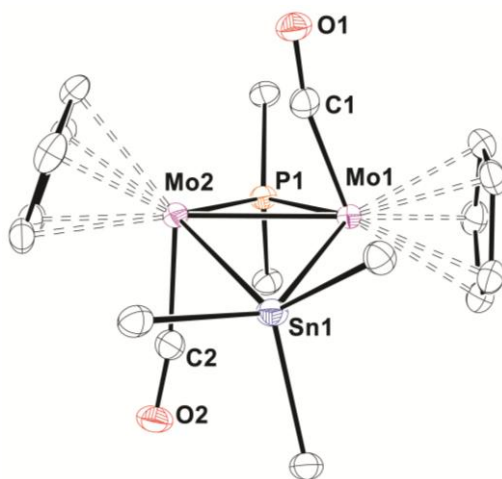


Figure 5. ORTEP diagram (30 % probability) of compound **6**, with H atoms, ^tBu and Ph groups (except C¹ atoms) omitted for clarity.

Table 6. Selected Bond Lengths (Å) and Angles (°) for Compound **6**.

Mo1–Mo2	2.5907(4)	Mo1–P–Mo2	64.87(2)
Mo1–P	2.4112(9)	Mo1–Sn–Mo2	52.243(8)
Mo2–P	2.4189(9)	C1–Mo1–Mo2	68.89(10)
Mo1–Sn	2.8770(4)	C2–Mo2–Mo1	92.47(10)
Mo2–Sn	3.0017(4)	P–Mo1–Sn	120.40(2)
Mo1–C1	1.923(3)	P–Mo2–Sn	115.49(2)

Mo2-C2	1.952(4)	P-Mo1-C1	76.98(8)
Mo2-C1	2.612(3)	P-Mo2-C2	91.28(11)
		Mo1-C1-O1	167.2(3)
		Mo2-C2-O2	170.7(3)

Spectroscopic data for **6** are fully consistent with the structure just discussed, although dynamic behavior is also evident. Thus, the IR spectrum agrees with the strong deviation of the CO ligands from ideal antiparallel arrangement found in the crystal, since it displays two strong stretching bands with relative intensities even more similar to each other than the ones observed for compounds **1** or **4**, and its ^{31}P NMR spectrum displays a quite deshielded resonance in the region expected for a P^tBu_2 ligand bridging a metal-metal triple bond, with a chemical shift (297 ppm) actually close to the value of the isoelectronic hydride **3**. However, as previously found for the chloride complex **1**, the ^1H and ^{13}C NMR spectra indicate apparent C_2 -symmetry, with one set of resonances for each pair of Cp and CO ligands. In order to explain this behavior we must propose the existence of a fast dynamic process in solution identical to that shown in Scheme 1 for the chloride complex, which would imply in this case the participation of an intermediate structure (not observed) with equivalent $\text{MoCp}(\text{CO})$ fragments and a flat central Mo_2PSn ring.

Photochemical Reactions of Agostic Alkyl Complexes 4. We have shown previously that removal of a CO ligand from the PCy_2 -bridged alkyls $[\text{M}_2\text{Cp}_2(\mu-\kappa^1:\eta^2\text{-CH}_2\text{R})(\mu\text{-PCy}_2)(\text{CO})_2]$ ($\text{M} = \text{Mo}$, $\text{R} = \text{H}$, Ph ; $\text{M} = \text{W}$, $\text{R} = \text{Ph}$) can be induced photochemically, yet the final outcome of these reactions depended critically on the nature of the alkyl group present. Thus, irradiation with UV-visible light of the methyl complex yielded mainly the monocarbonyl $[\text{Mo}_2\text{Cp}_2(\mu-\kappa^1:\eta^2\text{-CH}_3)(\mu\text{-PCy}_2)(\mu\text{-CO})]$, a compound displaying a stronger agostic interaction of the methyl group (according to DFT calculations).³⁵ However, this reaction was of little use from a synthetic point of view since: i) very long reaction times were required to achieve full conversions, ii) the product obtained was extremely air-sensitive, in fact being always accompanied by variable amounts of different oxo derivatives and, iii) attempted purification always led to its progressive decomposition. In contrast, irradiation of the Mo_2 and W_2 benzyl derivatives yielded directly the benzyldiene complexes $[\text{M}_2\text{Cp}_2(\mu\text{-CPh})(\mu\text{-PCy}_2)(\mu\text{-CO})]$ in a quite selective manner. These products follow from fast decarbonylation of the dimetallic unit and full dehydrogenation of the benzyl ligand through a multistep process for which no intermediates were detected.^{36, 11} Interestingly the irradiation of $[\text{Mo}_2\text{Cp}_2(\mu-\kappa^1:\eta^2\text{-CH}_3)(\mu\text{-PCy}_2)(\text{CO})_2]$ in presence of transition

metal complexes (*i.e.* $[\text{M}(\text{CO})_6]$, $[\text{Fe}_2(\text{CO})_9]$, etc.) yielded tri- or tetranuclear clusters bearing bridging methylidyne ($\mu\text{-CH}$) ligands, this proving that under photochemical conditions fast dehydrogenation of the CH_3 group might also be achieved, yet at that time we could not find any connection between the agostic monocarbonyl complex and the dehydrogenation products.^{35, 37} Taking into account these precedents, we resorted to study the photochemical behavior of the P^tBu_2 -bridged alkyl complexes **4a,b** to evaluate if the presence of a bulkier phosphanyl could exert any influence on the stability or evolution of these highly unsaturated species.

Irradiation with visible-UV light of hexane solutions of compound **4a** yielded the corresponding 30-electron methyl complex $[\text{Mo}_2\text{Cp}_2(\mu\text{-}\kappa^1\text{:}\eta^2\text{-CH}_3)(\mu\text{-P}^t\text{Bu}_2)(\mu\text{-CO})]$ (**7**) (Chart 2) in almost quantitative manner (as judged by NMR), in a reaction which is significantly faster than that of the related PCy_2 complex. The resulting solutions can be transferred to Schlenk tubes or J. Young-valved NMR tubes without apparent decomposition, so allowing for further studies on the reactivity of **7**, even if this compound could not be further purified due to its progressive decomposition. We were particularly interested in the dehydrogenation of this complex as a possible route to the corresponding methylidyne derivative, a reaction we could not test at the time for the corresponding PCy_2 -bridged complex, even if the corresponding product $[\text{Mo}_2\text{Cp}_2(\mu\text{-CH})(\mu\text{-PCy}_2)(\mu\text{-CO})]$ could be prepared through alternative (but more difficult) routes.³⁷ We have now found that moderate heating (353 K) of freshly prepared toluene solutions of **7** in a sealed NMR tube for 3 h yielded selectively the corresponding unsaturated methylidyne complex $[\text{Mo}_2\text{Cp}_2(\mu\text{-CH})(\mu\text{-P}^t\text{Bu}_2)(\mu\text{-CO})]$ (**8**) (Chart 2). We must note that such dehydrogenation of agostic alkyls has been rarely observed, although we can quote a couple of examples of related reactions (besides those reported by us), these involving $\mu\text{-CH}_3/\mu\text{-CH}$ transformations at either $[\text{Ru}_2]$ ³⁸ or $[\text{Fe}_3]$ ³⁹ complexes and a $\mu\text{-CH}_2\text{R}/\mu\text{-CH}/\mu\text{-CR}$ ($\text{R} = \text{CH}_2\text{Ph}$) transformation at a $[\text{Ru}_3]$ cluster.⁴⁰

As for the benzyl derivative **4b**, irradiation of its toluene solutions yielded the corresponding benzyldiyne complex $[\text{Mo}_2\text{Cp}_2(\mu\text{-CPh})(\mu\text{-P}^t\text{Bu}_2)(\mu\text{-CO})]$ (**9**) as expected (Chart 2). Interestingly, IR and NMR monitoring of this reaction allowed us to identify the formation of a sufficiently long-lived intermediate that accumulates in these solutions at the initial stages of the reaction, identified by an IR band at 1783 cm^{-1} . This intermediate evolved spontaneously over the course of 30 min at room temperature to give the final benzyldiyne product **9** with no further observable

intermediates. Fortunately, the use of short irradiation times and low temperature (243 K) yielded mixtures in which the mentioned intermediate is the main product, alongside the benzyldiyne **9**, this enabling its low-temperature spectroscopic characterization as the carbene hydride complex $[\text{Mo}_2\text{Cp}_2(\text{H})(\mu\text{-CHPh})(\mu\text{-P}^t\text{Bu}_2)(\mu\text{-CO})]$ (**10**) (Chart 2), a formulation also supported by DFT calculations (see below). As expected, when these solutions were allowed to reach room temperature, then a neat and progressive dehydrogenation of **10** to yield the benzyldiyne **9** was observed. The formation of a carbene hydride intermediate is, of course, a reasonable outcome after removal of a CO ligand from a complex already bearing an agostic alkyl group, since it is expected that the unsaturation thus generated can induce the cleavage of the agostic C–H bond.

Solution Structure of the Agostic Alkyl Complex 7. The available spectroscopic data for compound **7** are comparable to those of its PCy₂-analogue and therefore a similar structure is assumed,³⁵ a proposal also supported by DFT-calculations (Figure 6). The presence of just one bridging carbonyl ligand is denoted by the low-frequency stretching band (1715 cm⁻¹) observed in the IR spectrum and the highly deshielded ¹³C NMR resonance of this ligand (297 ppm). As also observed for the PCy₂-compound, a fluxional behavior is denoted by the ¹H and ¹³C NMR spectra, these displaying single resonances for the two Cp ligands and an averaged ¹H resonance for the three methyl protons (–1.92 ppm). These observations are in agreement with a rapid exchange of the environment of the H atoms within the Me group which also exchanges the metal atom involved in the agostic interaction, a situation mimicking that described above for its parent compound **4a** and remaining fast on the NMR timescale down to 183 K. A noteworthy spectroscopic feature for **7** is the strong deshielding of nearly 80 ppm operated on the ¹³C resonance of the bridging methyl ligand ($\delta_{\text{C}} = 41$ ppm), when compared to that of its parent 32-electron complex **4a** (–42 ppm). We have observed similar deshielding effects for bridging hydrides when comparing saturated and unsaturated complexes (*i.e.* $\delta_{\text{H}} = -7$ ppm for $[\text{Mo}_2\text{Cp}_2(\mu\text{-H})(\mu\text{-PCy}_2)(\text{CO})_2]$ ⁶ vs. –13 ppm for $[\text{Mo}_2\text{Cp}_2(\mu\text{-H})(\mu\text{-PCy}_2)(\text{CO})_4]$),¹⁸ hence we attribute the strong deshielding of the ¹³C methyl resonance in **7** to the strong magnetic anisotropy generated by its close proximity to the metal–metal triple bond (DFT-computed M–M = 2.481 Å). Finally, we note that the value of the averaged ¹J_{HC} measured for the methyl resonance (110 Hz) is significantly smaller than the one measured for its parent complex **4a** (126 Hz), actually being

even lower than that of the related PCy₂ compound (116 Hz),³⁵ then pointing to the presence of a quite strong agostic interaction of the bridging methyl group in **7**.⁴¹ This is also in agreement with the DFT-optimized structure of **7** (Figure 6), which displays a quite asymmetric α -agostic bridging methyl group (Mo–C1 = 2.195, 2.434 Å; C1–H = 1.157, 1.09 Å; see the Supporting Information) with a Mo2–H1 bond distance of 1.989 Å, a figure nearly 0.3 Å shorter than the corresponding distance computed at the same level for the dicarbonyl complex [Mo₂Cp₂(μ - κ^1 : η^2 -CH₃)(μ -PCy₂)(CO)₂] (*ca.* 2.30 Å).⁸

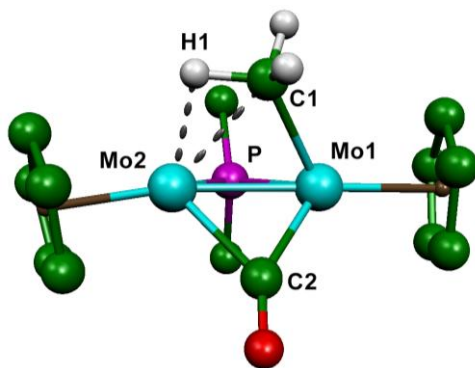


Figure 6. Optimized structure of compound **7** with H atoms (except methyl ones) and ^tBu groups (except C1 atoms) omitted for clarity. Selected bond lengths (Å): Mo1–Mo2 2.481, Mo1–C2 2.034, Mo2–C2 2.168, Mo1–C1 2.195, Mo2–C1 2.434, Mo2–H1 1.989, C1–H1 1.157, Mo1–P 2.445, Mo2–P 2.425.

Solution Structure of the Carbyne-Bridged Complexes. Structural characterization of the carbyne complexes **5**, **8** and **9** is facilitated by the similarity of their spectroscopic data (Table 2 and Experimental Section) with those of the large family of compounds [M₂Cp₂(μ -CR)(μ -PR₂)(μ -CO)] (M = Mo, W; R = H, Me, Ph, OMe, OEt, OP(O)(OPh)₂) which have been prepared previously by us and structurally characterized by X-ray crystallography in some cases. Then, a detailed discussion of these data is not required here. All these compounds display a highly deshielded ³¹P NMR resonance around 260 ppm, a figure consistent with the presence of phosphanyl ligands bridging across metal–metal triple bonds.¹⁸ Moreover, as expected for complexes with bridging carbynes, strongly deshielded ¹³C resonances for the bridgehead carbon atoms are observed in the ¹³C{¹H} NMR spectra, with their chemical shifts following the order Ph \approx H > OMe, as also found for the related PCy₂ complexes. The nature of the substituent at the

carbyne group is clearly evidenced by the ^1H NMR spectra; in particular, the methyldiylne complex **8** displays a diagnostic strongly deshielded resonance at 16.8 ppm (16.7 ppm in the PCy_2 complex), a situation which we have attributed previously to the strong anisotropy associated with the $\pi_{\text{Mo-C}}$ electron density.¹¹ Other spectroscopic data for these complexes are indicative of molecules having symmetry-related metal fragments, this requiring, for the methoxycarbyne complex **5**, fast rotation of the OMe group around the $\text{C}_{\text{carbyne}}\text{-O}$ bond in solution, a process otherwise observed in several PCy_2 -bridged methoxycarbyne complexes.²⁸

Solution Structure of the Carbene Hydride Complex 10. As noted above, the characterization of **10** is based on the spectroscopic data obtained from mixtures of this product with the benzylidene derivative **9**, yet the structure proposed for it also finds additional support from DFT calculations (Figure 7). The first evidence for the presence of a semibridging CO ligand in **10** comes from its IR spectrum, which displays a single C–O stretching band (1783 cm^{-1}) at frequencies significantly higher than those expected for bridging carbonyls (*cf.* 1715 cm^{-1} in **7**), in fact approaching the values measured for the hydride **3**. The semibridging coordination is also supported by the corresponding ^{13}C resonance (287 ppm), placed below the typical figures for symmetrical bridging carbonyls (*ca.* 300 ppm), but well above those of terminal ligands (*ca.* 250 ppm). The highly deshielded ^{31}P resonance (287.8 ppm) is consistent with the formulation of a metal-metal triple bond for this compound (DFT-computed Mo–Mo distance of 2.492 Å) and results comparable to that of the isoelectronic hydride **3** (289 ppm). However, the static structure presented in Chart 2 is incompatible with the available ^1H and ^{13}C NMR data, these being indicative of the existence of a symmetry plane relating both metal fragments. Thus, at all the temperatures the Cp groups give rise to a single resonance, while the ^tBu groups give rise to separate signals. Additionally, a single resonance is also found in the ^1H spectra (1.73 ppm) for the methylenic proton and the hydride ligand. This resonance correlates in a standard HSQC experiment with a broad ^{13}C resonance located at 130 ppm. The high chemical shift of the latter resonance certainly excludes the presence of a bridging alkyl ligand similar to that present in the methyl complex **7**, since this would be expected to give rise to a significantly more shielded resonance in the ^{13}C spectrum (*cf.* 40 ppm for **7**). Instead, such a chemical shift is comparable to the figures found for methylenic bridgehead carbon atoms, as the one in the complex $[\text{Mo}_2\text{Cp}_2(\mu\text{-CHPh})(\text{O})(\mu\text{-PCy}_2)(\text{NO})]^+$ ($\delta_{\text{C}} = 132\text{ ppm}$).⁴² The above observations can be explained by

assuming the operation of a fluxional process involving the rapid exchange of the methylenic proton and hydride positions through an intermediate structure with a bridging agostic alkyl ligand $[\text{Mo}_2\text{Cp}_2(\mu-\kappa^1:\eta^2\text{-CH}_2\text{Ph})(\mu\text{-P}^t\text{Bu}_2)(\mu\text{-CO})]$ (**7-Bz** in Scheme 3), a complex lying only $5.7 \text{ kJ}\cdot\text{mol}^{-1}$ above the carbene hydride **10** according to DFT calculations. We have computed that the fluxional process in **10** would actually take place through two transition states, the first one (**TS1-Bz**) involving the reductive elimination of hydride and carbene ligands to reach the alkyl-bridged intermediate **7-Bz** and located only $+26.0 \text{ kJ}\cdot\text{mol}^{-1}$ above the latter. Then, the exchange of benzylic hydrogen atoms would take place through a second low-energy transition **TS-Isom** having a non-agostic symmetrical benzyl-bridge and placed only $24.9 \text{ kJ}\cdot\text{mol}^{-1}$ above **7-Bz** (see Supporting Information), this being followed by the oxidative addition of the new agostic C–H bond to regenerate the hydride complex **10**.

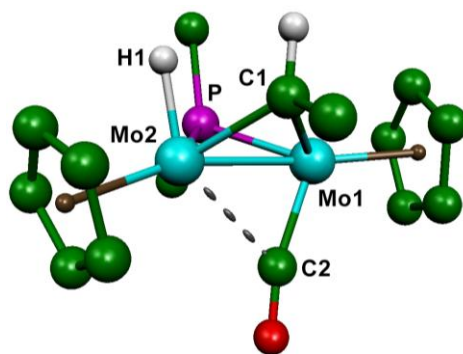
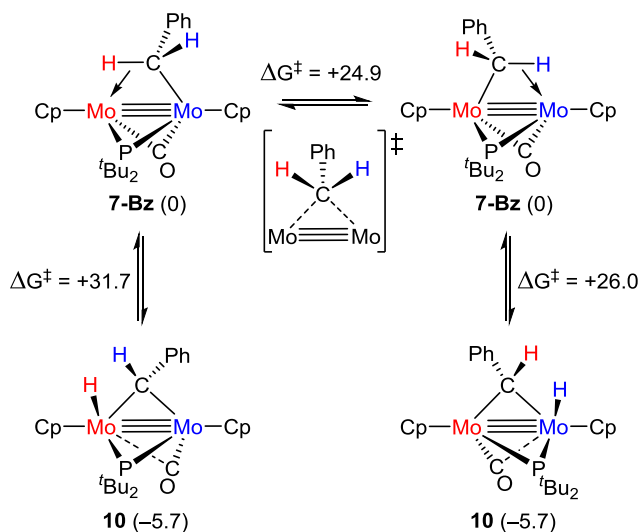


Figure 7. Optimized structure of compound **10** with H atoms (except hydride and carbene ones) and t Bu groups (except C1 atoms) omitted for clarity. Selected bond lengths (\AA): Mo1–Mo2 2.498, Mo1–C1 2.199, Mo2–C1 2.159, Mo1–C2 1.950, Mo2–C2 2.509, Mo2–H 1.673, Mo1–P 2.468, Mo2–P 2.427.

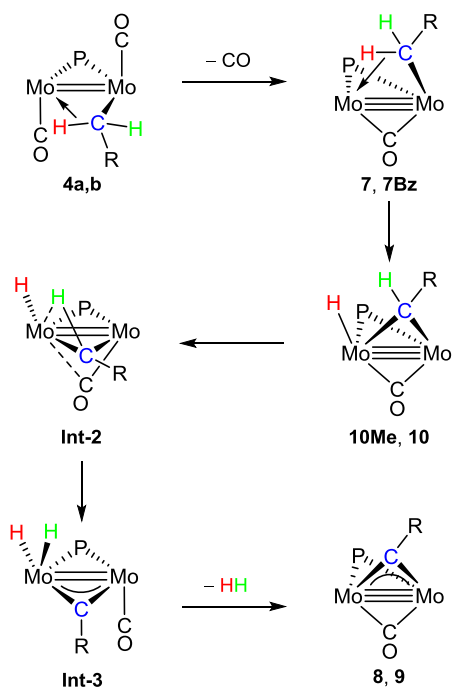


Scheme 3. Fluxional Process Proposed for Compound **10** in Solution, with Gibbs Free Energies (in $\text{kJ}\cdot\text{mol}^{-1}$) referenced to the energy of **7-Bz**.

Reaction Pathway for the Decarbonylation of Compounds 4a,b. The identification of compound **10** during the photolysis of the benzyl complex **4b** was a welcomed surprise, since no intermediates had been observed previously in the related reaction of the PCy_2 -bridged complex nor they are detected in the transformation of the agostic methyl **7** into the methylidyne **8**. Thus, we are now in a better position to depict a sensible reaction pathway for all these unusual transformations (Scheme 4). In order to provide additional support for our mechanistic proposal we have also carried out a complete DFT calculation of the reaction profiles for the methyl- and benzyl-bridged complexes, this providing valuable information to interpret the different experimental results (Figure 8). Thus, both reactions would be initiated by a photochemically-induced decarbonylation step yielding the corresponding 30-electron alkyl complexes $[\text{Mo}_2\text{Cp}_2(\mu-\kappa^1:\eta^2\text{-CH}_2\text{R})(\mu\text{-P}^t\text{Bu}_2)(\mu\text{-CO})]$ [$\text{R} = \text{H}$ (**7**), Ph (**7-Bz**)], which have been chosen as the energy reference for all the remaining computed species. This first step corresponds to a well-known behavior of dicarbonyl complexes of type $[\text{Mo}_2\text{Cp}_2(\mu\text{-PR}_2)(\mu\text{-X})(\text{CO})_2]$ ($\text{X} = \text{PR}_2$, CPh , COMe), which do not decarbonylate easily upon heating, but do it readily under UV irradiation. Although the resulting complex **7** is final product at room temperature for the methyl-bridged system, the analogous benzyl complex **7-Bz** was not observed experimentally as it would isomerize rapidly to yield the carbene hydride complex **10**, which is the only observable species preceding the final benzyldiyne product **9**. Our calculations indicate that in both systems the

overall dehydrogenation of the alkyl ligands in compounds **7** to form the corresponding carbyne derivatives ($\mathbf{7} \rightarrow \mathbf{8} + \text{H}_2$ and $\mathbf{7-Bz} \rightarrow \mathbf{9} + \text{H}_2$) are highly favorable processes from a thermodynamic point of view, with Gibbs free energies of reaction of -34 (Me) and -67 (Bz) $\text{kJ}\cdot\text{mol}^{-1}$. The different species observed experimentally in these reactions are also rationalized in view of the energetic profile depicted in Figure 8. Thus, in both cases the isomerization of the alkyls **7** into the corresponding carbene hydrides of type **10** would take place through a single transition state (**TS-1**) of low energy ($+43.7$ (Me) or $+26.0$ $\text{kJ}\cdot\text{mol}^{-1}$ (Bz)). However, while this transformation is thermodynamically favorable for the benzyl complex, with the observed carbene hydride compound **10** being nearly -5.7 $\text{kJ}\cdot\text{mol}^{-1}$ below the 30-electron alkyl complex, it is an uphill reaction (by $+18.4$ $\text{kJ}\cdot\text{mol}^{-1}$) for the methyl complex, thus making **10-Me** an unobservable species. The next step in these reactions is, in both systems, the rate-determining step and it involves a change in the coordination mode of the bridging carbene group in compounds **10** so as to adopt an agostic C–H \cdots M interaction involving the Mo atom already bearing the hydride ligand formed after the first C–H bond activation (**Int-2Me/Bz**). The change in the coordination mode of the carbene group is also accompanied by a strong rearrangement of the central Mo₂PC ring in these molecules, this reducing significantly the puckering of this ring. Such a strong rearrangement is surely related to the high energetic cost of this step as, otherwise, it would have been expected to involve a much modest activation energy, because it creates new C–H \cdots M interactions that reduce the unsaturated nature of the dimetal center. There are two additional points of relevance about these transformations. First, the presence of a bottleneck (in terms of energy requirement) in both reactions explain why compounds **7** and **10** are the only species observed after the initial decarbonylation step, since they are the most stable species located before the rate-determining step. Secondly, the overall reaction barriers established by these transition states of $+86$ (**TS-2Me**) and $+76$ (**TS-2Bz**) $\text{kJ}\cdot\text{mol}^{-1}$ agree with the observation of progressive transformation into the final carbyne product at room temperature of the benzyl derivative **10**, while such a transformation requires moderate heating in the case of the methyl complex **7**. In any case, once the agostic carbene intermediates **Int-2Me/Bz** are formed, then the second C–H oxidative addition take place rapidly involving a quite modest energetic cost through the transition states **TS-3Me/Bz** which are respectively located at $+50.0$ and $+26.2$ $\text{kJ}\cdot\text{mol}^{-1}$ above the respective precursors **7** and **10**. This generates intermediate carbyne complexes **Int-3Me/Bz** which display two hydride ligands located at the same metal and in close

proximity (*ca.* 1.76 Å), from which reductive elimination of dihydrogen can take place easily to yield the carbyne products eventually isolated in these reactions. Although we have not been able to locate the corresponding transition states for this latter step, relaxed potential energy surface scans for the H···H bond formation reaction in these intermediates proved that quite modest energy increases of *ca.* 42 kJ·mol⁻¹ are involved in the formation of the hydrogen molecule. It seems reasonable then to assume that, after formation of the H–H bond its elimination to give the 30-electron carbyne complexes **8** and **9** must take place essentially in a barrierless way because it is leading to thermodynamically quite stable products. We finally note that, while all the C–H bond cleavages required for dehydrogenation of the alkyl ligands in these complexes are kinetically accessible at room temperature or upon moderate heating, these elemental steps are thermodynamically favourable only for the benzyl-bridged system.



Scheme 4. Proposed Mechanism for the Formation of Carbyne Compounds **8** and **9**.

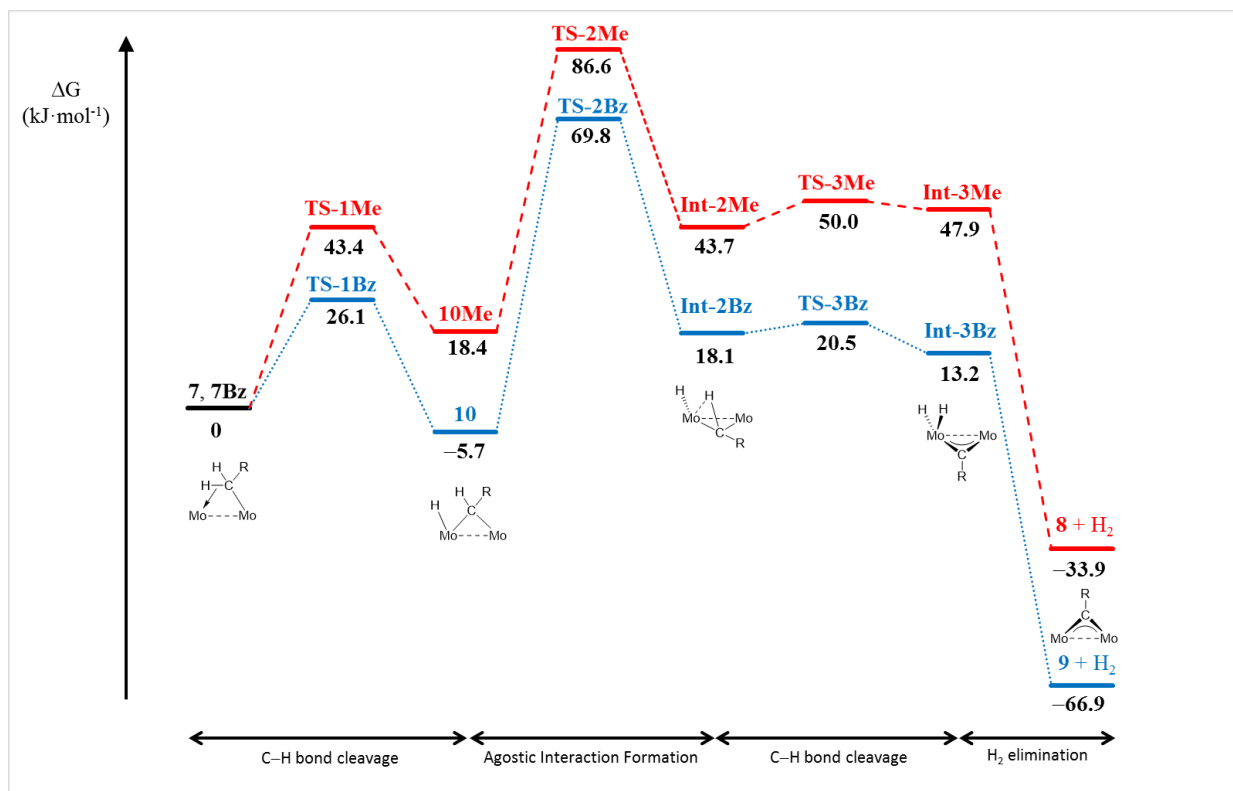


Figure 8. Computed kinetic profile for the dehydrogenation reactions leading to carbyne complexes **8** and **9**, with Gibbs free energies in kJ mol^{-1} .

Conclusions

The development of a synthetic route leading to the 30-electron anion $[\text{Mo}_2\text{Cp}_2(\mu\text{-P}^t\text{Bu}_2)(\mu\text{-CO})_2]^-$ (**2**) has allowed us to get access to new unsaturated hydride and alkyl derivatives bearing the sterically-demanding P^tBu_2 ligand. When confronted with different electrophiles (NH_4PF_6 , IMe , ClCH_2Ph , ClSnPh_3), anion **2** behaves in a way similar to related anions bearing sterically less demanding phosphanyl bridges, yet the presence of the bulky P^tBu_2 group indeed has significant effects on the structure and chemical behavior of some of the corresponding neutral derivatives. In the first place, the corresponding hydride complex $[\text{Mo}_2\text{Cp}_2(\text{H})(\mu\text{-P}^t\text{Bu}_2)(\text{CO})_2]$ displays a terminal hydride ligand both in solution and in the solid state, in contrast to the more conventional bridging coordination found in all related hydrides $[\text{Mo}_2\text{Cp}_2(\mu\text{-H})(\mu\text{-PR}_2)(\text{CO})_2]$ ($\text{R} = \text{Cy}, \text{Et}, \text{OEt}, \text{Ph}$). According to DFT calculations, the terminal and H-bridged isomers are almost isoenergetic in the case of the P^tBu_2 -bridged hydride and, in fact, taking into account solvation effects (PCM method) or van der Waals interactions forces (Grimme's dispersion correction) are key in order to reproduce the experimentally observed preference for the terminal

hydride coordination. An additional point of interest arising from these calculations is that, in spite of the different construction in terms of orbital components, the strength of the intermetallic bonding in these isomers is not greatly affected by the change in coordination mode of the hydride (terminal vs. bridging), as judged from the similar M–M bond lengths or electron densities accumulated at the intermetallic bond critical points. Secondly, as concerning the structures of dicarbonyl complexes of type $[\text{Mo}_2\text{Cp}_2(\mu\text{-X})(\mu\text{-PR}_2)(\text{CO})_2]$ ($X = \text{H}, \text{Cl}, \text{SnPh}_3$) we note that the presence of the bulkier P^tBu_2 ligand increases the degree of puckering of the central PMo_2X rings of these molecules, which is accompanied by a distortion of the carbonyls away from an antiparallel arrangement, with one of them leaning towards the intermetallic region in a linear semibridging way. Thirdly, as concerning agostic alkyl-bridged complexes $[\text{Mo}_2\text{Cp}_2(\mu\text{-}\kappa^1:\eta^2\text{-CH}_2\text{R})(\mu\text{-PR}_2)(\text{CO})_2]$, we found that replacement of PCy_2 with a P^tBu_2 phosphanyl ligand has several positive effects on the photochemical decarbonylation of the methyl complex, with the reaction now taking place significantly faster and in a much more selective way to give the 30-electron alkyl derivative $[\text{Mo}_2\text{Cp}_2(\mu\text{-}\kappa^1:\eta^2\text{-CH}_3)(\mu\text{-P}^t\text{Bu}_2)(\mu\text{-CO})]$. The higher stability of the latter complex (when compared to that of the related PCy_2 compound), allowed us to explore its thermal stability, to find that just a moderate heating can induce full dehydrogenation of the bridging alkyl to give the methylidyne derivative $[\text{Mo}_2\text{Cp}_2(\mu\text{-CH})(\mu\text{-P}^t\text{Bu}_2)(\mu\text{-CO})]$. In the case of the benzyl complex, a stabilizing effect of the P^tBu_2 bridge is evident in the low-temperature photochemical experiments, this allowing for the spectroscopic detection of a reaction intermediate preceding the dehydrogenation step and identified as the carbene hydride $[\text{Mo}_2\text{Cp}_2(\text{H})(\mu\text{-CHPh})(\mu\text{-P}^t\text{Bu}_2)(\text{CO})]$, a complex evolving spontaneously at room temperature to the final benzylidyne-bridged complex $[\text{Mo}_2\text{Cp}_2(\mu\text{-CPh})(\mu\text{-P}^t\text{Bu}_2)(\mu\text{-CO})]$ eventually isolated. The identification of the above carbene hydride intermediate has allowed us to depict a complete mechanism, fully supported on extensive DFT calculations, to explain the formation of the alkylidyne complexes, which would be initiated by the photochemically-induced decarbonylation that yields agostic intermediates $[\text{Mo}_2\text{Cp}_2(\mu\text{-}\kappa^1:\eta^2\text{-CH}_2\text{R})(\mu\text{-P}^t\text{Bu}_2)(\mu\text{-CO})]$, these then evolving thermally with subtle differences depending on R. Maybe surprisingly, the two C–H oxidative addition steps required for dehydrogenation of the alkyl ligands in these complexes take place on the same metal center and involve quite modest activation energies, while the rate-limiting step in both cases involves a change in the coordination mode of the carbene ligand to adopt an

agostic mode, a process which requires a substantial flattening of the central Mo₂CP ring of these molecules.

Experimental Section

General Procedures and Starting Materials. All manipulations and reactions were carried out under an argon (99.995%) atmosphere using standard Schlenk techniques. Solvents were purified according to literature procedures and distilled prior to use.⁴³ All the reagents were obtained from usual commercial suppliers and used as received, unless otherwise stated. Petroleum ether refers to that fraction distilling in the range 338-343 K. Filtrations were carried out through diatomaceous earth unless otherwise stated. Photochemical experiments were performed using jacketed Schlenk tubes, cooled by tap water (*ca.* 288 K) or by a closed 2-propanol circuit kept at the desired temperature with a cryostat. A 400 W mercury lamp placed *ca.* 1 cm away from the Schlenk tube was used for all experiments. Chromatographic separations were carried out using jacketed columns refrigerated by tap water (*ca.* 288 K) or by a closed 2-propanol circuit kept at the desired temperature with a cryostat. Commercial aluminum oxide (activity I, 70-290 mesh) was degassed under vacuum prior to use and then mixed under argon with the appropriate amount of degassed water to reach the activity desired (activity IV, unless otherwise stated). IR stretching frequencies of CO ligands were measured in solution (using CaF₂ windows), or in Nujol mulls (using NaCl windows), and are referred to as $\nu(\text{CO})(\text{solvent})$ and $\nu(\text{CO})(\text{Nujol})$, respectively. Nuclear magnetic resonance (NMR) spectra were routinely recorded at 400.13 (¹H), 162.12 (³¹P{¹H}) or 100.63 MHz (¹³C{¹H}), at 298 K in C₆D₆ solution unless otherwise stated. Chemical shifts (δ) are given in ppm, relative to internal tetramethylsilane (¹H, ¹³C) or external 85% aqueous H₃PO₄ (³¹P). Coupling constants (J) are given in Hertz.

Preparation of [Mo₂Cp₂(μ -Cl)(μ -P^tBu₂)(CO)₂] (1). In a typical experiment, a solution of [Mo₂Cp₂(CO)₆] (0.500 g, 1.02 mmol) and ClP^tBu₂ (245 μ L, 1.37 mmol) in 20 mL of xylene were refluxed under argon for 1 h and 15 min to give a dark green solution containing compound **1** in an essentially pure manner (as shown by ³¹P{¹H} NMR and IR). Unfortunately, all our attempts to isolate this complex as a bulk solid material were unsuccessful due to its progressive decomposition upon manipulation, this also preventing us from obtaining a satisfactory elemental analysis for this compound. However, removal of solvent from the reaction mixture

gave a crude green residue ready for further use. The crystals used in the X-ray diffraction study were grown by slow diffusion of a layer of petroleum ether in a saturated solution of the crude compound in toluene at 253 K. $\nu(\text{CO})(\text{xylene})$: 1891 (m), 1849 (vs) cm^{-1} . $\nu(\text{CO})(\text{THF})$: 1889 (m), 1846 (vs) cm^{-1} . $^{31}\text{P}\{^1\text{H}\}$ NMR: δ 215.9 (s). ^1H NMR: δ 4.98 (s, 10H, Cp), 1.23 (d, $J_{\text{HP}} = 13$, 18H, ^tBu).

Preparation of solutions of $\text{Li}[\text{Mo}_2\text{Cp}_2(\mu\text{-P}^t\text{Bu}_2)(\mu\text{-CO})_2]$ (2-Li). A solution of compound **1** (*ca.* 1 mmol) in tetrahydrofuran (15 mL) was stirred with an excess of $\text{Li}[\text{BHET}_3]$ (2.6 mL of a 1 M solution in THF, 2.60 mmol) for 30 min to give a red solution which was shown (by $^{31}\text{P}\{^1\text{H}\}$ NMR and IR) to contain essentially pure compound **2-Li** ready for further use. Attempts to obtain crystalline samples of this highly air-sensitive compound have been unsuccessful so far. $\nu(\text{CO})(\text{THF})$: 1656 (w), 1589 (m, sh), 1562 (vs) cm^{-1} . $^{31}\text{P}\{^1\text{H}\}$ NMR (121.49 MHz, $\text{THF-}d_8$): δ 240.3 (s). ^1H NMR (300.13 MHz, $\text{THF-}d_8$): δ 5.24 (s, 10H, Cp), 1.02 (d, $J_{\text{HP}} = 13$, 18H, ^tBu).

Preparation of solutions of $\text{Na}[\text{Mo}_2\text{Cp}_2(\mu\text{-P}^t\text{Bu}_2)(\mu\text{-CO})_2]$ (2-Na). METHOD A: A solution of compound **1** (*ca.* 1 mmol) in tetrahydrofuran (10 mL) was stirred with an excess of 0.5% Na-amalgam (*ca.* 1 mL, 3 mmol) for 30 min to give a red suspension that was transferred to another Schlenk tube using a cannula. METHOD B: A solution of compound **3** (0.050 g, 0.095 mmol) in tetrahydrofuran (10 mL) was stirred with an excess of 0.5% Na-amalgam (*ca.* 0.25 mL, 0.75 mmol) for 5 min to give a red suspension that was transferred to another Schlenk tube using a cannula. The suspensions thus obtained were shown to contain essentially pure compound **2-Na**, a salt poorly soluble in tetrahydrofuran, but ready for further use. Attempts to obtain crystalline samples of this highly air-sensitive compound have been unsuccessful so far. $\nu(\text{CO})(\text{THF})$: 1652 (w), 1588 (vs) cm^{-1} . The low-solubility of this salt in typical organic solvents precluded the collection of its NMR data.

Preparation of $[\text{Mo}_2\text{Cp}_2(\text{H})(\mu\text{-P}^t\text{Bu}_2)(\text{CO})_2]$ (3). A solution containing *ca.* 1 mmol of compound **2-Li** in tetrahydrofuran (15 mL), prepared as described above, was stirred with excess $(\text{NH}_4)\text{PF}_6$ (*ca.* 0.25 g, 1.53 mmol) for 30 min to give a dark green solution. The solvent was then removed under vacuum and the residue was extracted with toluene-petroleum ether (1:4) and chromatographed through an alumina column at 253 K. Elution with toluene-petroleum ether (1:1) gave a green fraction yielding, after removal of solvents under vacuum, compound **3** as a

green solid (0.455 g, 85% overall yield from $[\text{Mo}_2\text{Cp}_2(\text{CO})_6]$). The crystals used in the X-ray diffraction study were grown by the slow diffusion of a layer of petroleum ether into a concentrated toluene solution of the complex at room temperature. Anal. Calcd for $\text{C}_{20}\text{H}_{29}\text{Mo}_2\text{O}_2\text{P}$: C, 45.82; H, 5.58; Found: C, 45.59; H, 5.51. $\nu(\text{CO})(\text{petroleum ether})$: 1825 (s), 1794 (vs) cm^{-1} . $\nu(\text{CO})(\text{THF})$: 1813 (s), 1778 (vs) cm^{-1} . $^{31}\text{P}\{^1\text{H}\}$ NMR (Tol- d_8): δ 288.6 (s). $^{31}\text{P}\{^1\text{H}\}$ NMR (Tol- d_8 , 173 K): δ 287.6 (s). ^1H NMR (Tol- d_8): δ 4.98 (s, 10H, Cp), 1.25 (d, $J_{\text{HP}} = 13$, 18H, ^tBu), -2.48 (d, $J_{\text{HP}} = 31$, 1H, Mo–H). ^1H NMR (Tol- d_8 , 173 K): δ 4.90, 4.81 (2s, 2 x 5H, Cp), 1.20 (s, br, 9H, ^tBu), 1.05 (d, $J_{\text{HP}} = 10$, 9H, ^tBu), -2.54 (d, $J_{\text{HP}} = 31$, 1H, Mo–H). $^{13}\text{C}\{^1\text{H}\}$ NMR (Tol- d_8): δ 264.5 (s, CO), 90.8 (s, Cp), 44.3 [d, $J_{\text{CP}} = 10$, $\text{C}^1(^t\text{Bu})$], 33.5 [d, $J_{\text{CP}} = 3$, $\text{C}^2(^t\text{Bu})$]. $^{13}\text{C}\{^1\text{H}\}$ NMR (Tol- d_8 , 173 K): δ 271.0, 264.4 (2s, br, CO), 91.0, 90.6 (2s, Cp), 45.3, 42.3 [2s, br, $\text{C}^1(^t\text{Bu})$], 32.4 [s, br, $2\text{C}^2(^t\text{Bu})$].

Preparation of $[\text{Mo}_2\text{Cp}_2(\mu-\kappa^1:\eta^2\text{-CH}_3)(\mu\text{-P}^t\text{Bu}_2)(\text{CO})_2]$ (4a**).** A suspension containing *ca.* 1 mmol of compound **2-Na** in tetrahydrofuran (15 mL), prepared by the method A described above, was stirred with excess *i*Me (750 μL , 12.1 mmol) for 3 h to give a brown-reddish solution. The solvent was then removed under vacuum and the residue was extracted with dichloromethane-petroleum ether (1:4) and chromatographed through an alumina column at 253 K. Elution with the same solvent mixture gave a brown fraction yielding, after removal of solvents under vacuum, compound **4a** as a brown solid (0.340 g, 62% overall yield from $[\text{Mo}_2\text{Cp}_2(\text{CO})_6]$). Elution with dichloromethane-petroleum ether (4:1) gave an orange fraction yielding, after removal of solvents under vacuum, compound $[\text{Mo}_2\text{Cp}_2(\mu\text{-COMe})(\mu\text{-P}^t\text{Bu}_2)(\mu\text{-CO})]$ (**5**) as an orange-red solid (0.064 g, 12% overall yield from $[\text{Mo}_2\text{Cp}_2(\text{CO})_6]$). Anal. Calcd for $\text{C}_{21}\text{H}_{31}\text{Mo}_2\text{O}_2\text{P}$ (**4a**): C, 46.85; H, 5.80; Found: C, 46.74; H, 5.45. Anal. Calcd for $\text{C}_{21}\text{H}_{31}\text{Mo}_2\text{O}_2\text{P}$ (**5**): C, 46.85; H, 5.80; Found: C, 46.68; H, 5.75. *Spectroscopic data for 4a*: $\nu(\text{CO})(\text{petroleum ether})$: 1883 (m), 1835 (vs) cm^{-1} . $\nu(\text{CO})(\text{THF})$: 1869 (m), 1823 (vs) cm^{-1} . $^{31}\text{P}\{^1\text{H}\}$ NMR (121.49 MHz): δ 209.4 (s). ^1H NMR (300.13 MHz): δ 4.85 (d, $J_{\text{HP}} = 1$, 10H, Cp), 1.34 (d, $J_{\text{HP}} = 13$, 18H, ^tBu), -0.74 (d, $J_{\text{HP}} = 3$, $J_{\text{HC}} = 126$, 3H, $\mu\text{-CH}_3$). $^{13}\text{C}\{^1\text{H}\}$ NMR (75.47 MHz): δ 252.6 (d, $J_{\text{CP}} = 12$, CO), 89.1 (s, Cp), 43.9 [d, $J_{\text{CP}} = 12$, $\text{C}^1(^t\text{Bu})$], 33.8 [d, $J_{\text{CP}} = 4$, $\text{C}^2(^t\text{Bu})$], -42.3 (d, $J_{\text{CP}} = 3$, $\mu\text{-CH}_3$). *Spectroscopic data for 5*: $\nu(\text{CO})(\text{petroleum ether})$: 1718 (s) cm^{-1} . $\nu(\text{CO})(\text{CH}_2\text{Cl}_2)$: 1673 (s) cm^{-1} . $^{31}\text{P}\{^1\text{H}\}$ NMR (121.49 MHz): δ 259.0 (s). ^1H NMR (300.13 MHz): δ 5.66 (s, 10H, Cp), 3.29 (s, 3H, OMe), 0.92, 0.79 (2d, $J_{\text{HP}} = 14$, 2 x 9H, ^tBu). $^{13}\text{C}\{^1\text{H}\}$ NMR (CD_2Cl_2): δ 353.6 (d,

$J_{CP} = 14$, μ -COMe), 304.1 (d, $J_{CP} = 8$, μ -CO), 93.9 (s, Cp), 66.2 (s, OCH₃), 42.4 [d, $J_{CP} = 10$, C¹(^tBu)], 41.0 [d, $J_{CP} = 11$, C¹(^tBu)], 34.5, 33.8 [2d, $J_{CP} = 4$, C²(^tBu)].

Preparation of [Mo₂Cp₂(μ - κ^1 : η^2 -CH₂Ph)(μ -P^tBu₂)(CO)₂] (4b). A suspension containing *ca.* 0.100 mmol of compound **2-Na** in tetrahydrofuran (10 mL), prepared by the method B described above, was stirred overnight with an excess ClCH₂Ph (110 μ L, 0.960 mmol) to give a deep brown solution. The solvent was then removed under vacuum and the residue was extracted with dichloromethane-petroleum ether (1:4) and chromatographed through an alumina column. Elution with the same solvent mixture gave a brown fraction yielding, after removal of solvents under vacuum, compound **4b** as a brown solid (0.048 g, 78%). Anal. Calcd for C₂₇H₃₅Mo₂O₂P: C, 52.78; H, 5.74. Found: C, 52.49; H, 5.26. ν (CO)(petroleum ether): 1901 (m), 1843 (vs) cm⁻¹. ν (CO)(toluene): 1889 (m), 1834 (vs) cm⁻¹. ³¹P{¹H} NMR (121.49 MHz): δ 204.6 (s). ¹H NMR (300.13 MHz): δ 7.32 (m, 2H, Ph), 7.03 (m, 3H, Ph), 4.85 (s, 10H, Cp), 2.59 (d, $J_{HH} = 15$, 1H, CH₂), 1.32 (d, $J_{HP} = 13$, 18H, ^tBu), -1.94 (dd, $J_{HH} = 15$, $J_{HP} = 4$, 1H, CH₂). ¹³C{¹H} NMR (75.47 MHz): δ 251.9 (d, $J_{CP} = 11$, CO), 154.0 [s, C¹(Ph)], 127.9, 127.3 [2s, C^{2,3}(Ph)], 122.6 [s, C⁴(Ph)], 89.0 (s, Cp), 44.0 [d, $J_{CP} = 12$, C¹(^tBu)], 33.7 [d, $J_{CP} = 4$, C²(^tBu)], -3.5 (s, μ -CH₂Ph).

Preparation of [Mo₂Cp₂(μ -P^tBu₂)(μ -SnPh₃)(CO)₂] (6). A suspension containing *ca.* 0.050 mmol of compound **2-Na** in tetrahydrofuran (10 mL), prepared by the method B described above, was stirred with ClSnPh₃ (0.020 g, 0.050 mmol) for 5 min to give a green solution. The solvent was then removed under vacuum and the residue was extracted with dichloromethane-petroleum ether (1:3) and chromatographed through an alumina column at 253 K. Elution with the same solvent mixture gave a green fraction yielding, after removal of solvents under vacuum, compound **6** as a dark green solid (0.037 g, 85%). The crystals used in the X-ray diffraction study were grown by the slow diffusion of layers of petroleum ether and toluene into a concentrated dichloromethane solution of the complex at 253 K. Anal. Calcd for C₃₈H₄₃Mo₂O₂PSn: C, 52.26; H, 4.96; Found: C, 51.88; H, 5.05. ν (CO)(dichloromethane): 1866 (m), 1796 (vs) cm⁻¹. ν (CO)(THF): 1870 (m), 1802 (vs) cm⁻¹. ³¹P{¹H} NMR (121.49 MHz, CD₂Cl₂): δ 297.4 (s, $J_{P-117Sn} \approx J_{P-119Sn} \approx 82$). ¹H NMR (300.13 MHz, CD₂Cl₂): δ 7.55-7.24 (m, 15H, Ph), 4.70 (s, 10H, Cp), 1.50 (d, $J_{HP} = 14$, 18H, ^tBu). ¹³C{¹H} NMR (75.47 MHz, CD₂Cl₂): δ 252.1 (d, $J_{CP} = 11$, CO), 145.9 [s, $J_{C-117Sn} = 328$, $J_{C-119Sn} = 342$, C¹(Ph)], 137.7 [s, $J_{P-117Sn} \approx J_{P-119Sn} \approx 82$].

$^{119}\text{Sn} \approx 36$, $\text{C}^2(\text{Ph})$], 128.2 [s, $J_{\text{P-}^{117}\text{Sn}} \approx J_{\text{P-}^{119}\text{Sn}} \approx 42$, $\text{C}^3(\text{Ph})$], 127.6 [s, $J_{\text{P-}^{117}\text{Sn}} \approx J_{\text{P-}^{119}\text{Sn}} \approx 9$, $\text{C}^4(\text{Ph})$], 90.3 (s, Cp), 48.0 [d, $J_{\text{CP}} = 10$, $\text{C}^1(\text{tBu})$], 33.3 [d, $J_{\text{CP}} = 3$, $\text{C}^2(\text{tBu})$].

Preparation of solutions of $[\text{Mo}_2\text{Cp}_2(\mu-\kappa^1:\eta^2\text{-CH}_3)(\mu\text{-P}^t\text{Bu}_2)(\mu\text{-CO})]$ (7). A petroleum ether solution (10 mL) of compound **4a** (0.020 g, 0.037 mmol) was irradiated with visible–UV light in a Pyrex Schlenk flask for 20 min with a gentle N_2 (99.9995%) purge to give a brown-reddish solution containing compound **7** as essentially unique product. Unfortunately, all our attempts to isolate this complex as a solid material were unsuccessful due to its progressive decomposition upon manipulation, this also preventing us from obtaining a satisfactory elemental analysis for this compound. $\nu(\text{CO})(\text{petroleum ether})$: 1715 (s) cm^{-1} . $^{31}\text{P}\{^1\text{H}\}$ NMR: δ 266.2 (s). $^{31}\text{P}\{^1\text{H}\}$ NMR ($\text{Tol-}d_8$): δ 265.0 (s). ^1H NMR: δ 5.60 (s, 10H, Cp), 1.02 (d, $J_{\text{HP}} = 12$, 9H, ^tBu), 0.42 (d, $J_{\text{HP}} = 12$, 9H, ^tBu), -1.92 (s, $J_{\text{HC}} = 110$, 3H, $\mu\text{-CH}_3$). ^1H NMR ($\text{Tol-}d_8$, 223 K): δ 5.49 (s, 10H, Cp), 0.94 (d, $J_{\text{HP}} = 14$, 9H, ^tBu), 0.36 (d, $J_{\text{HP}} = 13$, 9H, ^tBu), -1.92 (s, 3H, $\mu\text{-CH}_3$). $^{13}\text{C}\{^1\text{H}\}$ NMR ($\text{Tol-}d_8$, 223 K): δ 296.7 (s, $\mu\text{-CO}$), 94.4 (s, Cp), 45.6 [d, $J_{\text{CP}} = 7$, $\text{C}^1(\text{tBu})$], 44.2 [d, $J_{\text{CP}} = 14$, $\text{C}^1(\text{tBu})$], 41.3 (d, $J_{\text{CP}} = 6$, $\mu\text{-CH}_3$), 34.3 [d, $J_{\text{CP}} = 4$, $\text{C}^2(\text{tBu})$], 32.8 [d, $J_{\text{CP}} = 5$, $\text{C}^2(\text{tBu})$].

Preparation of $[\text{Mo}_2\text{Cp}_2(\mu\text{-CH})(\mu\text{-P}^t\text{Bu}_2)(\mu\text{-CO})]$ (8). A freshly prepared solution of compound **7** (*ca.* 0.037 mmol) in toluene- d_8 (0.5 mL) was transferred to a J-Young NMR tube and heated at 353 K for 3 h to give a pink-reddish solution. The solvent was then removed under vacuum and the residue was extracted with dichloromethane-petroleum ether (1:8) and chromatographed through an alumina column. Elution with dichloromethane-petroleum ether (1:4) gave a pink-reddish fraction yielding, after removal of solvents under vacuum, compound **8** as a red solid (0.014 g, 75%). Anal. Calcd for $\text{C}_{20}\text{H}_{29}\text{Mo}_2\text{OP}$: C, 47.26; H, 5.75; Found: C, 47.00; H, 5.84. $\nu(\text{CO})(\text{petroleum ether})$: 1726 (s) cm^{-1} . $\nu(\text{CO})(\text{dichloromethane})$: 1684 (s) cm^{-1} . $^{31}\text{P}\{^1\text{H}\}$ NMR: δ 258.6 (s). ^1H NMR: δ 16.83 (s, 1H, $\mu\text{-CH}$), 5.68 (s, 10H, Cp), 0.85, 0.70 (2d, $J_{\text{HP}} = 14$, 2 x 9H, ^tBu). $^{13}\text{C}\{^1\text{H}\}$ NMR: δ 383.1 (d, $J_{\text{CP}} = 15$, $\mu\text{-CH}$), 297.7 (d, $J_{\text{CP}} = 9$, $\mu\text{-CO}$), 94.4 (s, Cp), 42.0 [d, $J_{\text{CP}} = 12$, $\text{C}^1(\text{tBu})$], 37.5 [d, $J_{\text{CP}} = 10$, $\text{C}^1(\text{tBu})$], 34.6 [d, $J_{\text{CP}} = 5$, $\text{C}^2(\text{tBu})$], 33.8 [d, $J_{\text{CP}} = 4$, $\text{C}^2(\text{tBu})$].

Preparation of $[\text{Mo}_2\text{Cp}_2(\mu\text{-CPh})(\mu\text{-P}^t\text{Bu}_2)(\mu\text{-CO})]$ (9). A petroleum ether solution (10 mL) of compound **4b** (0.025 g, 0.041 mmol) was irradiated with visible–UV light in a quartz Schlenk flask for 30 min with a gentle N_2 (99.9995%) purge, and then allowed to stir for 20 min at room

temperature to give a dark red solution. The solvent was then removed under vacuum and the residue was extracted with dichloromethane-petroleum ether (1:1) and chromatographed through an alumina column. Elution with dichloromethane-petroleum ether (2:1) gave a red fraction yielding, after removal of solvents under vacuum, compound **9** as a red solid (0.022 g, 92%). Anal. Calcd for C₂₆H₃₃Mo₂OP: C, 53.44; H, 5.69; Found: C, 53.19; H, 5.46. $\nu(\text{CO})(\text{toluene})$: 1726 (s) cm⁻¹. $\nu(\text{CO})(\text{dichloromethane})$: 1686 (s) cm⁻¹. ³¹P{¹H} NMR (CD₂Cl₂): δ 265.2 (s). ¹H NMR (CD₂Cl₂): δ 7.13 (false t, $J_{\text{HH}} = 8$, 2H, Ph), 7.01 (t, $J_{\text{HH}} = 7$, 1H, Ph), 6.61 (false d, $J_{\text{HH}} = 7$, 2H, Ph), 5.84 (s, 10H, Cp), 0.95 (d, $J_{\text{HP}} = 14$, 18H, ^tBu). ¹³C{¹H} NMR (CD₂Cl₂): δ 385.9 (d, $J_{\text{CP}} = 14$, μ -CPh), 302.4 (d, $J_{\text{CP}} = 9$, μ -CO), 161.8 [s, C¹(Ph)], 127.8 [s, C³(Ph)], 125.0 [s, C⁴(Ph)], 122.1 [s, C²(Ph)], 96.0 (s, Cp), 43.2 [d, $J_{\text{CP}} = 12$, C¹(^tBu)], 39.7 [d, $J_{\text{CP}} = 10$, C¹(^tBu)], 34.5, 34.1 [2d, $J_{\text{CP}} = 4$, C²(^tBu)].

Preparation of solutions of [Mo₂Cp₂(H)(μ -CHPh)(μ -P^tBu₂)(CO)] (10**).** A petroleum ether solution (15 mL) of compound **4b** (0.025 g, 0.041 mmol) was irradiated with visible–UV light in a quartz Schlenk flask at 243 K for 20 min with a gentle N₂ (99.9995%) purge to give a dark red solution shown by NMR to contain a mixture of **10** and **9** in a *ca.* 3:2 ratio. Compound **10** is thermally unstable in solution and it is completely transformed into **9** upon stirring these mixtures at room temperature for 15–30 min. $\nu(\text{CO})(\text{petroleum ether})$: 1783 (s) cm⁻¹. ³¹P{¹H} NMR (CD₂Cl₂, 253 K): δ 287.8 (s). ¹H NMR (CD₂Cl₂, 253 K): δ 7.17 (false t, $J_{\text{HH}} = 8$, 2H, Ph), 7.05 (t, $J_{\text{HH}} = 7$, 1H, Ph), 6.78 (false d, $J_{\text{HH}} = 7$, 2H, Ph), 5.40 (s, 10H, Cp), 1.73 (d, $J_{\text{HP}} = 13$, 2H, μ -CHPh + Mo–H), 1.45, 0.77 (2d, $J_{\text{HP}} = 14$, 2 x 9H, ^tBu). ¹³C{¹H} NMR (CD₂Cl₂, 253 K): δ 287.6 (s, μ -CO), 160.8 [s, C¹(Ph)], 131.3 (s, br, μ -CHPh), 127.7 [s, C³(Ph)], 127.0 [s, C⁴(Ph)], 123.2 [s, C²(Ph)], 93.9 (s, Cp), 45.2 [d, $J_{\text{CP}} = 9$, C¹(^tBu)], 44.7 [d, $J_{\text{CP}} = 13$, C¹(^tBu)], 33.7 [d, $J_{\text{CP}} = 4$, C²(^tBu)], 33.4 [bs, C²(^tBu)].

DFT Calculations. All DFT computations were carried out using the Gaussian03 or Gaussian09 packages,⁴⁴ in which the hybrid method B3LYP was used with the Becke three-parameter exchange functional⁴⁵ and the Lee–Yang–Parr correlation functional.⁴⁶ An accurate numerical integration grid (99,590) was used for all the calculations via the keyword Int = Ultrafine. Effective core potentials and their associated double- ζ LANL2DZ basis set were used for the metal atoms.⁴⁷ The light elements (P, O, C, and H) were described with the 6-31G* basis.⁴⁸ Geometry optimizations were performed under no symmetry restrictions, and frequency analyses

were performed for all the stationary points to ensure that minimum structures with no imaginary frequencies were achieved. Transition states were optimized through the Synchronous Transit-Guided Quasi-Newton (STQN) Method as implemented in Gaussian, characterized by frequency analysis (one imaginary frequency) and their connectivity was corroborated through Intrinsic-Reaction-Coordinate (IRC) calculations. Atoms-in-Molecules Analysis was carried out using the MultiWFN program.⁴⁹ Solvent effects (dichloromethane, $\epsilon = 8.93$) were modelled using the polarized-continuum-model of Tomasi and co-workers (PCM),²⁹ by using the gas-phase optimized structures. Empirical dispersion corrections developed by Grimme and co-workers were also used to evaluate the energetic ordering of isomers **3T** and **3B**.³⁰

X-ray Structure Determination of Compounds 1 and 6. Data collection were performed at 150 K on an Oxford Diffraction Xcalibur Nova single crystal diffractometer, using Cu K α radiation ($\lambda = 1.5418 \text{ \AA}$). Images were collected at a 62 mm fixed crystal-detector distance, using the oscillation method, with 1.0° (**1**) or 1.20° (**6**) oscillation and variable exposure time per image (1.0-3 (**1**) and 3.5-10 s (**6**)). Data collection strategy was calculated with the program CrysAlis Pro CCD,⁵⁰ and data reduction and cell refinement was performed with the program CrysAlis Pro RED.⁵⁰ An empirical absorption correction was applied using the SCALE3 ABSPACK algorithm as implemented in the latter program. Using the program suite WINGX,⁵¹ the structure was solved by Patterson interpretation and phase expansion using SHELXL2016,⁵² and refined with full-matrix least squares on F^2 using SHELXL2016 to give the residuals collected in Table S10. All non-hydrogen atoms were refined anisotropically, and all hydrogen atoms were geometrically placed and refined using a riding model. In the case of compound **1** Friedel pairs were not measured separately and, hence, absolute configuration cannot be determined.

X-ray Structure Determination of Compound 3. The X-ray data were collected on a Kappa-Appex-II Bruker diffractometer using graphite-monochromated MoK α radiation at 100 K. The software APEX⁵³ was used for collecting frames with ω/ϕ scans measurement method. The SAINT software was used for the data reduction,⁵⁴ and a multi-scan absorption correction was applied with SADABS.⁵⁵ The structure was solved by Patterson interpretation and phase expansion using SHELXL 2016,⁵² and refined with full-matrix least squares on F^2 using SHELXL 2016⁵² to give the residuals collected in Table S10. All the positional parameters and

the anisotropic temperature factors of all non-H atoms were refined anisotropically and all hydrogen atoms were geometrically placed and refined using a riding model, except for H(1) which was located in the Fourier Maps and refined isotropically. After convergence, the strongest residual peaks (3.31 and 1.38 e A⁻³) were close to Mo(1) and Mo(2) atoms, respectively.

ASSOCIATED CONTENT

A CIF file containing full crystallographic data for compounds **1**, **3** and **6** (CCDC 1552066-1552068). A PDF file containing results of DFT calculations (drawings, orbitals and energies) and NMR spectra of selected complexes. An XYZ file including the Cartesian coordinates for all computed species. This material is available free of charge via the Internet at <http://pubs.acs.org>.

AUTHOR INFORMATION

Corresponding Authors

* Email: garciavdaniel@uniovi.es (DGV), mara@uniovi.es (M.A.R.)

Notes

The authors declare no competing financial interest.

ACKNOWLEDGMENT

We thank the Gobierno del Principado de Asturias (Project GRUPIN14-011) and the MINECO of Spain and FEDER for financial support (Project CTQ2015-63726-P), the CMC of the Universidad de Oviedo for access to computing facilities and, the X-ray diffraction services at the Universidad de Oviedo and Universidad de Santiago de Compostela (Spain) for the acquisition of the diffraction data used in this work.

REFERENCES

1. (a) Power, P. P. Some highlights from the development and use of bulky monodentate ligands. *J. Organomet. Chem.* **2004**, *689*, 3904-3919. (b) Kays, D. L. Recent developments

- in transition metal diaryl chemistry. *Dalton Trans.* **2011**, *40*, 769-778. (c) Chmely, S. C.; Hanusa, T. P. Complexes with Sterically Bulky Allyl Ligands: Insights into Structure and Bonding. *Eur. J. Inorg. Chem.* **2010**, 1321-1337. (d) Agnew-Francis, K. A.; Williams, C. M. Catalysts Containing the Adamantane Scaffold. *Adv. Synth. Catal.* **2016**, *358*, 675-700.
- Nguyen, T.; Sutton, A. D.; Brynda, M.; Fetting, J. C.; Long, G. J.; Power, P. P. Synthesis of a Stable Compound with Fivefold Bonding Between Two Chromium(I) Centers. *Science* **2005**, *310*, 844-847.
 - (a) Noor, A.; Kempe, R. M5M – Key compounds of the research field metal–metal quintuple bonding. *Inorg. Chim. Acta* **2015**, *424*, 75-82. (b) Nair, A. K.; Harisomayajula, N. V. S.; Tsai, Y.-C. The lengths of the metal-to-metal quintuple bonds and reactivity thereof. *Inorg. Chim. Acta* **2015**, *424*, 51-62. (c) Nair, A. K.; Harisomayajula, N. V. S.; Tsai, Y.-C. Theory, synthesis and reactivity of quintuple bonded complexes. *Dalton Trans.* **2014**, *43*, 5618-5638. (d) Hua, S.-A.; Tsai, Y.-C.; Peng, S.-M. A Journey of Metal-metal Bonding beyond Cotton's Quadruple Bonds. *J. Chin. Chem. Soc.* **2014**, *61*, 9-26. (e) Harisomayajula, N. V. S.; Nair, A. K.; Tsai, Y.-C. Discovering complexes containing a metal-metal quintuple bond: from theory to practice. *Chem. Commun.* **2014**, *50*, 3391-3412. (f) Noor, A.; Kempe, R. The shortest metal-metal bond. *Chem. Rec.* **2010**, *10*, 413-416. (g) Ni, C.; Power, P. P. In *Metal-Metal Bonding*; Parkin, G., Ed.; Springer Berlin Heidelberg: Berlin, Heidelberg, 2010; pp 59-111. (h) Wagner, F. R.; Noor, A.; Kempe, R. Ultrashort metal-metal distances and extreme bond orders. *Nat. Chem.* **2009**, *1*, 529-536.
 - (a) Tolman, C. A. Steric effects of phosphorus ligands in organometallic chemistry and homogeneous catalysis. *Chem. Rev.* **1977**, *77*, 313-348. (b) Schier, A.; Schmidbaur, H. In *Encyclopedia of Inorganic Chemistry*; John Wiley & Sons, Ltd: 2006.
 - García-Vivó, D.; Ramos, A.; Ruiz, M. A. Cyclopentadienyl and related complexes of the group 6 elements having metal–metal triple bonds: Synthesis, structure, bonding and reactivity. *Coord. Chem. Rev.* **2013**, *257*, 2143-2191.
 - (a) García, M. E.; Melón, S.; Ramos, A.; Riera, V.; Ruiz, M. A.; Belletti, D.; Graiff, C.; Tiripicchio, A. A Versatile and Unprecedented Triply Bonded Dimolybdenum Carbonyl Anion. *Organometallics* **2003**, *22*, 1983-1985. (b) García, M. E.; Melón, S.; Ramos, A.; Ruiz, M. A. Synthesis of the triply-bonded dimolybdenum anions $[\text{Mo}_2(\eta^5\text{-C}_5\text{H}_5)_2(\mu\text{-PA}_2)(\mu\text{-CO})_2]^-$ (A = Cy, Et, Ph, OEt): unsaturated hydride and carbyne derivatives. *Dalton Trans.* **2009**, 8171-8182.
 - Alvarez, M. A.; García, M. E.; García-Vivó, D.; Ruiz, M. A.; Vega, M. F. Synthesis and Reactivity of the Triply Bonded Binuclear Anion $[\text{W}_2(\eta^5\text{-C}_5\text{H}_5)_2(\mu\text{-PCy}_2)(\mu\text{-CO})_2]^-$: Tungsten Makes a Difference. *Organometallics* **2010**, *29*, 512-515.
 - García, M. E.; Ramos, A.; Ruiz, M. A.; Lanfranchi, M.; Marchio, L. Structure and Bonding in the Unsaturated Hydride- and Hydrocarbyl-Bridged Complexes $[\text{Mo}_2(\eta^5\text{-C}_5\text{H}_5)_2(\mu\text{-X})(\mu\text{-PCy}_2)(\text{CO})_2]$ (X = H, CH₃, CH₂Ph, Ph). Evidence for the Presence of α -Agostic and π -Bonding Interactions. *Organometallics* **2007**, *26*, 6197-6212.
 - Alvarez, M. A.; García, M. E.; García-Vivó, D.; Ruiz, M. A.; Vega, M. F. Hydride, gold(I) and related derivatives of the unsaturated ditungsten anion $[\text{W}_2\text{Cp}_2(\mu\text{-PCy}_2)(\mu\text{-CO})_2]^-$. *Dalton Trans.* **2014**, *43*, 16044-16055.
 - We adopted here a “half-electron” counting convention for complexes having (μ -H) ligands or related groups as SnR₃, so that compound $[\text{M}_2\text{Cp}_2(\mu\text{-H})(\mu\text{-P}^t\text{Bu}_2)(\text{CO})_2]$ is regarded as having a Mo–Mo triple bond. Other authors recommend the adoption of a “half-arrow” convention for this sort of molecules (M. L. H. Green, G. Parkin, *Struct. Bond.* **2017**, *117*,

79-140 and references therein). Under such convention, however, the above complexes should be assimilated to the corresponding halide-bridged complexes $[\text{Mo}_2\text{Cp}_2(\mu\text{-X})(\mu\text{-PR}_2)(\text{CO})_2]$ (Chart 1), therefore being formulated with double M–M bonds, a relationship which we consider of little use to interpret the strong differences separating the structure and spectroscopic properties of all these molecules.

11. Alvarez, M. A.; García, M. E.; García-Vivó, D.; Martínez, M. E.; Ruiz, M. A. Binuclear Carbyne and Ketenyl Derivatives of the Alkyl-Bridged Complexes $[\text{Mo}_2(\eta^5\text{-C}_5\text{H}_5)_2(\mu\text{-CH}_2\text{R})(\mu\text{-PCy}_2)(\text{CO})_2]$ (R = H, Ph). *Organometallics* **2011**, *30*, 2189-2199.
12. Alvarez, M. A.; García, M. E.; Ramos, A.; Ruiz, M. A. Reactivity of the Unsaturated Hydride $[\text{Mo}_2(\eta^5\text{-C}_5\text{H}_5)_2(\mu\text{-H})(\mu\text{-PCy}_2)(\text{CO})_2]$ toward P-Donor Bidentate Ligands and Unsaturated N-Containing Organic Molecules. *Organometallics* **2007**, *26*, 1461-1472.
13. Adatia, T.; McPartlin, M.; Mays, M. J.; Morris, M. J.; Raithby, P. R. Chemistry of phosphido-bridged dimolybdenum complexes. Part 3. Reinvestigation of the reaction between $[\text{Mo}_2(\eta\text{-C}_5\text{H}_5)_2(\text{CO})_6]$ and P_2Ph_4 ; X-ray structures of $[\text{Mo}_2(\eta\text{-C}_5\text{H}_5)_2(\mu\text{-PPh}_2)_2(\text{CO})_2]$, $[\text{Mo}_2(\eta\text{-C}_5\text{H}_5)_2(\mu\text{-PPh}_2)_2(\mu\text{-CO})]$, and *trans*- $[\text{Mo}_2(\eta\text{-C}_5\text{H}_5)_2(\mu\text{-PPh}_2)_2\text{O}(\text{CO})]$. *J. Chem. Soc., Dalton Trans.* **1989**, 1555-1564.
14. Hey-Hawkins, E.; Fromm, K. Mixed-valence dinuclear molybdenum complexes: Synthesis and molecular structure of $(\text{Cp}^\circ\text{Mo})_2(\mu\text{-Cl})_n(\mu\text{-PPh}_2)_{3-n}$ (n = 1, 0; $\text{Cp}^\circ = \eta^5\text{-C}_5\text{Me}_4\text{Et}$). *Polyhedron* **1995**, *14*, 2027-2035.
15. Cabon, N.; Petillon, F. Y.; Schollhammer, P.; Talarmin, J.; Muir, K. W. Reaction of BH_4^- with $\{\text{Mo}_2\text{Cp}_2(\mu\text{-SMe})_n\}$ species to give tetrahydroborato, hydrido or dimetallaborane compounds: control of product by ancillary ligands. *Dalton Trans.* **2004**, 2708-2719.
16. Braterman, P. S. *Metal Carbonyl Spectra*. Academic Press: New York, 1975.
17. Alvarez, M. A.; García, M. E.; Ramos, A.; Ruiz, M. A. Dimolybdenum–Tin Derivatives of the Unsaturated Hydride $[\text{Mo}_2(\eta^5\text{-C}_5\text{H}_5)_2(\mu\text{-H})(\mu\text{-PCy}_2)(\text{CO})_2]$ and HSnR_3 (R = Ph, Bu): Bridging versus Terminal Coordination of the Triorganostannyl Group. *Organometallics* **2006**, *25*, 5374-5380.
18. García, M. E.; Riera, V.; Ruiz, M. A.; Rueda, M. T.; Sáez, D. Dimolybdenum and Ditungsten Cyclopentadienyl Carbonyls with Electron-Rich Phosphido Bridges. Synthesis of the Hydrido Phosphido Complexes $[\text{M}_2\text{Cp}_2(\mu\text{-H})(\mu\text{-PRR}')(\text{CO})_4]$ and Unsaturated Bis(phosphido) Complexes $[\text{M}_2\text{Cp}_2(\mu\text{-PR}_2)(\mu\text{-PR}'\text{R}'')(\text{CO})_x]$ (x = 1, 2; R, R', R'' = Et, Cy, ^tBu). *Organometallics* **2002**, *21*, 5515-5525.
19. Jones, R. A.; Schwab, S. T.; Stuart, A. L.; Whittlesey, B. R.; Wright, T. C. Synthesis of dinuclear phosphido or arsenido bridged complexes of molybdenum via reaction of secondary phosphines or arsines with $[\text{Mo}(\eta^5\text{-C}_5\text{H}_5)(\text{CO})_3]_2$: X-ray structures of $\{[\text{Mo}(\eta^5\text{-C}_5\text{H}_5)(\text{CO})_2]_2(\mu\text{-H})(\mu\text{-ER}_2)\}$ (E = P, R = ^tBu; or E = As, R = Me). *Polyhedron* **1985**, *4*, 1689-1695.
20. (a) Darensbourg, M. Y. Ion Pairing Effects on Transition Metal Carbonyl Anions. *Prog. Inorg. Chem.* **2007**, 221-274. (b) Darensbourg, M. Y.; Ash, C. E. Anionic Transition Metal Hydrides. *Adv. Organomet. Chem.* **1987**, Volume 27, 1-50.
21. Alvarez, M. A.; García, M. E.; Martínez, M. E.; Ramos, A.; Ruiz, M. A.; Sáez, D.; Vaissermann, J. M–P versus M–M Bonds as Protonation Sites in the Organophosphido-Bridged Complexes $[\text{M}_2\text{Cp}_2(\mu\text{-PR}_2)(\mu\text{-PR}'_2)(\text{CO})_2]$, (M = Mo, W; R, R' = Ph, Et, Cy). *Inorg. Chem.* **2006**, *45*, 6965-6978.
22. Crabtree, R. H.; Lavin, M. Structural analysis of the semibridging carbonyl. *Inorg. Chem.* **1986**, *25*, 805-812.

23. (a) Falvello, L. R.; Foxman, B. M.; Murillo, C. A. Fitting the Pieces of the Puzzle: The δ Bond. *Inorg. Chem.* **2014**, *53*, 9441-9456. (b) Liddle, S. T., Ed. *Molecular Metal-Metal Bonds*. Wiley-VCH:Weinheim: Germany, 2015.
24. Green, J. C.; Green, M. L. H.; Parkin, G. The occurrence and representation of three-centre two-electron bonds in covalent inorganic compounds. *Chem. Commun.* **2012**, *48*, 11481-11503.
25. (a) Suss-Fink, G.; Therrien, B. Dinuclear ruthenium and osmium arene trihydrido complexes: Versatile water-soluble synthons in organometallic chemistry. *Organometallics* **2007**, *26*, 766-774. (b) Koga, N.; Morokuma, K. Ab-Initio Study on the Structure and H₂ Dissociation Reaction of a Tetrahydride-Bridged Dinuclear Ru Complex, (C₅H₅)Ru(μ -H)₄Ru(C₅H₅). *J. Mol. Struct.* **1993**, *300*, 181-189. (c) Jezowska-Trzebiatowska, B.; Nissen-Sobocinska, B. Nature of the Hydrogen Bridge in Transition-Metal Complexes .2. Molecular-Orbital Calculations of Binuclear Carbonyls of Mn, Re, Cr, Mo and W with Double Hydrogen Bridges. *J. Organomet. Chem.* **1988**, *342*, 215-233.
26. Baik, M. H.; Friesner, R. A.; Parkin, G. Theoretical investigation of the metal-metal interaction in dimolybdenum complexes with bridging hydride and methyl ligands. *Polyhedron* **2004**, *23*, 2879-2900.
27. Bader, R. F. W. *Atoms in Molecules: A Quantum Theory*. Oxford University Press: Oxford, 1990.
28. García, M. E.; García-Vivó, D.; Ruiz, M. A.; Alvarez, S.; Aullón, G. Chemistry of unsaturated group 6 metal complexes with bridging hydroxy and methoxycarbonyl ligands. 1. Synthesis, structure, and bonding of 30-electron complexes. *Organometallics* **2007**, *26*, 4930-4941.
29. (a) Tomasi, J.; Mennucci, B.; Cammi, R. Quantum Mechanical Continuum Solvation Models. *Chem. Rev.* **2005**, *105*, 2999-3094. (b) Cossi, M.; Scalmani, G.; Rega, N.; Barone, V. New developments in the polarizable continuum model for quantum mechanical and classical calculations on molecules in solution. *J. Chem. Phys.* **2002**, *117*, 43-54.
30. Grimme, S. Semiempirical GGA-type density functional constructed with a long-range dispersion correction. *J. Comput. Chem.* **2006**, *27*, 1787-1799.
31. Alvarez, C. M.; Alvarez, M. A.; García, M. E.; Ramos, A.; Ruiz, M. A.; Lanfranchi, M.; Tiripicchio, A. A Triply Bonded Dimolybdenum Hydride Complex with Acid, Base and Radical Activity. *Organometallics* **2005**, *24*, 7-9.
32. Liu, X.-Y.; Ruiz, M. A.; Lanfranchi, M.; Tiripicchio, A. Phosphonate-Stannylenes Coupling in the Reactions of the Anion [Mn₂{ μ -OP(OEt)₂}{ μ -P(OEt)₂}(CO)₆}²⁻ with SnR₂Cl₂ (R = Bu, Ph). *Organometallics* **2005**, *24*, 3527-3531.
33. Ugrinov, A.; Sevov, S. C. Rationally Functionalized Deltahedral Zintl Ions: Synthesis and Characterization of [Ge₉-ER₃]³⁻, [R₃E-Ge₉-ER₃]²⁻, and [R₃E-Ge₉-Ge₉-ER₃]⁴⁻ (E = Ge, Sn; R = Me, Ph). *Chem. Eur. J.* **2004**, *10*, 3727-3733.
34. Alvarez, M. A.; García, M. E.; García-Vivó, D.; Ruiz, M. A.; Vega, M. F. Reactions of the Unsaturated Tungsten Anion [W₂Cp₂(μ -PCy₂)(μ -CO)₂]⁻ with C- and P-Based Electrophiles. *Organometallics* **2015**, *34*, 870-878.
35. Alvarez, M. A.; García-Vivó, D.; García, M. E.; Martínez, M. E.; Ramos, A.; Ruiz, M. A. Reactivity of the α -Agostic Methyl Bridge in the Unsaturated Complex [Mo₂(η^5 -C₅H₅)₂(μ - η^1 : η^2 -CH₃)(μ -PCy₂)(CO)₂]: Migratory Behavior and Methylidyne Derivatives. *Organometallics* **2008**, *27*, 1973-1975.

36. Alvarez, M. A.; García, M. E.; Martínez, M. E.; Menéndez, S.; Ruiz, M. A. Dehydrogenative Formation and Reactivity of the Unsaturated Benzylidyne-Bridged Complex $[\text{Mo}_2\text{Cp}_2(\mu\text{-CPh})(\mu\text{-PCy}_2)(\mu\text{-CO})]$: C–C and C–P Coupling Reactions. *Organometallics* **2010**, *29*, 710-713.
37. Alvarez, M. A.; García, M. E.; Martínez, M. E.; Ruiz, M. A. Heterometallic Derivatives of the Unsaturated Methyl-Bridged Complex $[\text{Mo}_2(\eta^5\text{-C}_5\text{H}_5)_2(\mu\text{-CH}_3)(\mu\text{-PCy}_2)(\text{CO})_2]$. Photochemical Generation of Methylidyne-Bridged Clusters. *Organometallics* **2010**, *29*, 904-916.
38. Connelly, N. G.; Forrow, N. J.; Gracey, B. P.; Knox, S. A. R.; Orpen, A. G. Activation of μ -alkylidene ligands through oxidation-deprotonation: a new synthesis of μ -methyne, and its hydrogenation to μ -methyl. *J. Chem. Soc., Chem. Commun.* **1985**, 14-16.
39. Dutta, T. K.; Vites, J. C.; Jacobsen, G. B.; Fehlner, T. P. The making and breaking of carbon-hydrogen bonds on a metal cluster framework. Analysis of the tautomerization and deprotonation of $\text{Fe}_3(\text{CO})_9\text{CH}_4$ leading to the interconversion of FeHFe and CHFe interactions. *Organometallics* **1987**, *6*, 842-847.
40. Tenjimbayashi, R.-I.; Murotani, E.; Takemori, T.; Takao, T.; Suzuki, H. Synthesis, structure, and property of a triruthenium cluster having a μ -alkyl ligand: Transformation of a $\mu_3(\perp)$ -alkyne ligand into a μ -alkyl ligand via a μ_3 -vinylidene complex. *J. Organomet. Chem.* **2007**, *692*, 442-454.
41. By assuming a value of 130 Hz for the C-H coupling in a regular bond, then the averaged figure of 110 Hz implies a value of 70 Hz for the C-H coupling in the agostic bond of 7, in the low extreme of the usual range of 75-100 Hz for agostic bonds. See Brookhart, M.; Green, M. L. H. *J. Organomet. Chem.* **1983**, *250*, 395-408.
42. Alvarez, M. A.; García, M. E.; García-Vivó, D.; Menéndez, S.; Ruiz, M. A. Electronic Structure and Reactivity of the Carbyne-Bridged Dimolybdenum Radical $[\text{Mo}_2(\eta^5\text{-C}_5\text{H}_5)_2(\mu\text{-CPh})(\mu\text{-PCy}_2)(\mu\text{-CO})]^\dagger$. *Organometallics* **2013**, *32*, 218-231.
43. Armarego, W. L. F.; Chai, C. L. L. *Purification of Laboratory Chemicals*. 7th ed.; Butterworth-Heinemann: Burlington, UK, 2012, 2012.
44. (a) Frisch, M. J.; Trucks, G. W.; Schlegel, H. B.; Scuseria, G. E.; Robb, M. A.; Cheeseman, J. R.; Montgomery, J. A.; Vreven, T.; Kudin, K. N.; Burant, J. C.; Millam, J. M.; Iyengar, S. S.; Tomasi, J.; Barone, V.; Mennucci, B.; Cossi, M.; Scalmani, G.; Rega, N.; Petersson, G. A.; Nakatsuji, H.; Hada, M.; Ehara, M.; Toyota, K.; Fukuda, R.; Hasegawa, J.; Ishida, M.; Nakajima, T.; Honda, Y.; Kitao, O.; Nakai, H.; Klene, M.; Li, X.; Knox, J. E.; Hratchian, H. P.; Cross, J. B.; Bakken, V.; Adamo, C.; Jaramillo, J.; Gomperts, R.; Stratmann, R. E.; Yazyev, O.; Austin, A. J.; Cammi, R.; Pomelli, C.; Ochterski, J. W.; Ayala, P. Y.; Morokuma, K.; Voth, G. A.; Salvador, P.; Dannenberg, J. J.; Zakrzewski, V. G.; Dapprich, S.; Daniels, A. D.; Strain, M. C.; Farkas, O.; Malick, D. K.; Rabuck, A. D.; Raghavachari, K.; Foresman, J. B.; Ortiz, J. V.; Cui, Q.; Baboul, A. G.; Clifford, S.; Cioslowski, J.; Stefanov, B. B.; Liu, G.; Liashenko, A.; Piskorz, P.; Komaromi, I.; Martin, R. L.; Fox, D. J.; Keith, T.; Laham, A.; Peng, C. Y.; Nanayakkara, A.; Challacombe, M.; Gill, P. M. W.; Johnson, B.; Chen, W.; Wong, M. W.; Gonzalez, C.; Pople, J. A., Gaussian 03, Revision D.01. In 2003. (b) Frisch, M. J.; Trucks, G. W.; Schlegel, H. B.; Scuseria, G. E.; Robb, M. A.; Cheeseman, J. R.; Scalmani, G.; Barone, V.; Mennucci, B.; Petersson, G. A.; Nakatsuji, H.; Caricato, M.; Li, X.; Hratchian, H. P.; Izmaylov, A. F.; Bloino, J.; Zheng, G.; Sonnenberg, J. L.; Hada, M.; Ehara, M.; Toyota, K.; Fukuda, R.; Hasegawa, J.; Ishida, M.; Nakajima, T.; Honda, Y.; Kitao, O.; Nakai, H.; Vreven, T.; Montgomery, J. A.; Peralta, J.

- E.; Ogliaro, F.; Bearpark, M.; Heyd, J. J.; Brothers, E.; Kudin, K. N.; Staroverov, V. N.; Kobayashi, R.; Normand, J.; Raghavachari, K.; Rendell, A.; Burant, J. C.; Iyengar, S. S.; Tomasi, J.; Cossi, M.; Rega, N.; Millam, J. M.; Klene, M.; Knox, J. E.; Cross, J. B.; Bakken, V.; Adamo, C.; Jaramillo, J.; Gomperts, R.; Stratmann, R. E.; Yazyev, O.; Austin, A. J.; Cammi, R.; Pomelli, C.; Ochterski, J. W.; Martin, R. L.; Morokuma, K.; Zakrzewski, V. G.; Voth, G. A.; Salvador, P.; Dannenberg, J. J.; Dapprich, S.; Daniels, A. D.; Farkas; Foresman, J. B.; Ortiz, J. V.; Cioslowski, J.; Fox, D. J., Gaussian 09, Revision B.01. In Wallingford CT, 2009.
45. Becke, A. D. Density- functional thermochemistry. III. The role of exact exchange. *J. Chem. Phys.* **1993**, *98*, 5648-5652.
 46. Lee, C.; Yang, W.; Parr, R. G. Development of the Colle-Salvetti correlation-energy formula into a functional of the electron density. *Phys. Rev. B* **1988**, *37*, 785-789.
 47. Hay, P. J.; Wadt, W. R. Ab initio effective core potentials for molecular calculations. Potentials for K to Au including the outermost core orbitals. *J. Chem. Phys.* **1985**, *82*, 299-310.
 48. (a) Hariharan, P. C.; Pople, J. A. The influence of polarization functions on molecular orbital hydrogenation energies. *Theor. Chim. Acta* **1973**, *28*, 213-222. (b) Petersson, G. A.; Al- Laham, M. A. A complete basis set model chemistry. II. Open- shell systems and the total energies of the first- row atoms. *J. Chem. Phys.* **1991**, *94*, 6081-6090. (c) Petersson, G. A.; Bennett, A.; Tensfeldt, T. G.; Al- Laham, M. A.; Shirley, W. A.; Mantzaris, J. A complete basis set model chemistry. I. The total energies of closed- shell atoms and hydrides of the first- row elements. *J. Chem. Phys.* **1988**, *89*, 2193-2218.
 49. Lu, T.; Chen, F. Multiwfn: A multifunctional wavefunction analyzer. *J. Comput. Chem.* **2012**, *33*, 580-592.
 50. *CrysAlis Pro*. Oxford Diffraction Limited, Ltd.: 2006.
 51. (a) Farrugia, L. WinGX suite for small-molecule single-crystal crystallography. *J. Appl. Crystallogr.* **1999**, *32*, 837-838. (b) Farrugia, L. WinGX and ORTEP for Windows: an update. *J. Appl. Crystallogr.* **2012**, *45*, 849-854.
 52. (a) Sheldrick, G. Crystal structure refinement with SHELXL. *Acta Crystallogr. Sect. C* **2015**, *71*, 3-8. (b) Sheldrick, G. A short history of SHELX. *Acta Crystallogr. Sect. A* **2008**, *64*, 112-122.
 53. *APEX 2, version 2.0-1*. Bruker AXS, Inc.: Madison: WI, 2005.
 54. *SMART & SAINT Software Reference Manuals, Version 5.051 (Windows NT Version)*. Bruker AXS, Inc.: Madison: WI, 1998.
 55. Sheldrick, G. M. *SADABS, Program for Empirical Absorption Correction*. University of Göttingen: Göttingen, Germany, 1996.

(For Table of Contents Use Only)

Table of Contents Synopsis

We present a high yield route for the preparation of the 30-electron anion $[\text{Mo}_2\text{Cp}_2(\mu\text{-P}^t\text{Bu}_2)(\mu\text{-CO})_2]^-$ having a bulky P^tBu_2 -bridge. This anion is a key entry point into the chemistry of different unsaturated hydride and hydrocarbyl complexes stabilized by this bulky bridging group, which also has significant effects on the structure and chemical behaviour of these species.

Graphics for Table of Contents

